

***E. coli* glycogen branching enzyme restores synthesis of starch-like polyglucans in an *Arabidopsis* mutant devoid of endogenous starch branching enzymes**

**Running Title:** Synthesis of starch-like polyglucans by *E. coli* BE

Laura Boyer <sup>1</sup>, Xavier Roussel <sup>1</sup>, Adeline Courseaux <sup>1</sup>, Ofilia Mvundza Ndjindji <sup>2,3</sup>,  
Christine Lancelon-Pin <sup>2,3</sup>, Jean-Luc Putaux <sup>2,3</sup>, Ian Tetlow <sup>4</sup>, Michael Emes <sup>4</sup>, Bruno  
Pontoire <sup>5</sup>, Christophe D'Hulst <sup>1</sup> and Fabrice Wattebled <sup>1,\*</sup>

<sup>1</sup> Unité de Glycobiologie Structurale et Fonctionnelle, UMR8576 CNRS – Université de  
Lille, F-59655 Villeneuve d'Ascq cedex, France

<sup>2</sup> Université Grenoble Alpes, Centre de Recherches sur les Macromolécules Végétales  
(CERMAV), F-38000 Grenoble, France

<sup>3</sup> CNRS, CERMAV, F-38000 Grenoble, France

<sup>4</sup> Department of Molecular and Cellular Biology, Science Complex, University of Guelph,  
Guelph, Ontario N1G 2W1, Canada

<sup>5</sup> UR1268 BIA, INRA, F-44300 Nantes, France

\* Corresponding author: [fabrice.wattebled@univ-lille1.fr](mailto:fabrice.wattebled@univ-lille1.fr)

Total word count: 7740

## ABSTRACT

Starch synthesis requires several enzymatic activities including branching enzymes (BEs) responsible for the formation of  $\alpha(1\rightarrow6)$  linkages. Distribution and number of these linkages are further controlled by debranching enzymes (DBEs) that cleave some of them, rendering the polyglucan water-insoluble and semi-crystalline. Although the activity of BEs and DBEs is mandatory to sustain normal starch synthesis, the relative importance of each in the establishment of the plant storage polyglucan (i.e. water-insolubility, crystallinity, presence of amylose) is still debated. Here, we have substituted the activity of BEs in *Arabidopsis* with that of the *Escherichia coli* glycogen branching enzyme (GlgB). The latter is the BE counterpart in the metabolism of glycogen, a highly branched water-soluble and amorphous storage polyglucan. GlgB was expressed in the *be2 be3* double mutant of *Arabidopsis* that is devoid of BE activity and consequently free of starch. The synthesis of a water-insoluble, partly crystalline, amylose-containing starch-like polyglucan was restored in GlgB-expressing plants, suggesting that BEs only have a limited impact on establishing essential characteristics of starch. Moreover, the balance between branching and debranching is crucial for the synthesis of starch, as an excess of branching activity results in the formation of highly branched, water-soluble, poorly crystalline polyglucan.

## KEYWORDS

Starch, glycogen,  $\alpha$ -glucan, polyglucan, branching enzyme, GlgB, *Arabidopsis thaliana*, *Escherichia coli*, debranching enzyme.

## INTRODUCTION

Amylopectin is one of the two homopolymers of glucose that constitute native starch in plants and algae. It is chemically identical to the glycogen found in bacteria, fungi and animals and is composed of glucosyl residues linked by  $\alpha(1\rightarrow4)$  O-glycosidic bonds and branched in  $\alpha(1\rightarrow6)$  linkages. However, the degree of branching of amylopectin does not exceed 5-6%, while it usually reaches 8 to 10% in glycogen (Buleon *et al.*, 1998; Roach *et al.*, 2012). Moreover, the distribution of  $\alpha(1\rightarrow6)$  linkages is different in both polyglucans. In glycogen, branch points are regularly distributed in the macromolecule, leading to the formation of a spherical homogenous structure with limited size (Melendez-Hevia *et al.*, 1993). On the other hand, amylopectin exhibits a heterogeneous molecular organization in which short linear segments are clustered and branch points form amorphous lamellae. Several models of cluster pattern have been proposed (Bertoft, 2013). Hizukuri's model suggests that clusters follow one another linearly. The clusters are linked together by longer glucans that expand from the preceding structure to the following (Hizukuri, 1986). More recently, Bertoft has proposed an alternative model in which clusters are linked side by side to a long, linear, glucan backbone (Bertoft, 2004). In Bertoft's model, the formation of a new cluster does not depend on the synthesis of a previous one. Regardless of which amylopectin model is considered, these differences between amylopectin and glycogen lead to different properties for both polymers. Amylopectin is water-insoluble and partly crystalline whereas glycogen is water-soluble and amorphous.

The biosynthesis of these polysaccharides involves the same set of enzymatic activities:

- i. Polymerizing enzymes (i.e. starch- or glycogen-synthases) that transfer the glucose moiety of a nucleotide-sugar (being ADP-glucose or UDP-glucose) to the non-reducing end of an  $\alpha$ -glucan by creating  $\alpha(1\rightarrow4)$  linkages (Fujita *et al.*, 2012).
- ii. Branching enzymes (1,4- $\alpha$ -glucan:1,4- $\alpha$ -glucan 6-glucosyltransferase; EC 2.4.1.18) that introduce the  $\alpha(1\rightarrow6)$  branch points by rearranging linear glucans. These enzymes cleave an  $\alpha(1\rightarrow4)$  linkage and then transfer the released glucan in  $\alpha(1\rightarrow6)$  position by an intermolecular or intramolecular mechanism (Tetlow, 2012).

However, in the case of amylopectin, an additional activity is required to allow the formation of the specific structure of this macromolecule: an isoamylase-type debranching enzyme removes some of the  $\alpha(1\rightarrow6)$  linkages created by branching enzymes. This step appears mandatory since mutants lacking isoamylases exhibit a severe reduction in starch content and accumulate large amounts of a highly branched water-soluble and amorphous polyglucan called phytoglycogen (Mouille *et al.*, 1996; Myers *et al.*, 2000; Ball *et al.*, 2003; Wattebled *et al.*, 2005). Compared to wild-type starch, phytoglycogen displays significant modifications of chain length distribution characterized by enrichment in very short chains (DP 3-5). The crystallization of the polysaccharide clearly depends on the distribution of  $\alpha(1\rightarrow6)$  linkages, but also on chain length distribution (Pfister *et al.*, 2014). Starch synthases (by elongating glucans) and isoamylases (by removing some branch points) are key enzymes that control both parameters that are crucial to define the final structure and properties of starch. Modification of plant BE activity level can affect the physicochemical characteristics of starch as well. For instance, the reduction of branching enzyme activity in potato by the antisense inhibition of both SBE A and SBE B induces the



synthesis of very-high-amylose starch in potato tubers (Schwall *et al.*, 2000). In rice and maize, modification of BE activity (by mutation or over-expression) alters the structure and properties of the endosperm starch (Sato *et al.*, 2003; Tanaka *et al.*, 2004; Yao *et al.*, 2004). Although it is obvious that BEs are mandatory for the synthesis of starch since these enzymes are the only one that create the  $\alpha(1\rightarrow6)$  linkages, their actual contribution for the determination of starch characteristics (i.e. water-insolubility, semi-crystallinity, presence of amylose, amylopectin DP<sub>max</sub> at 12-13) has not been precisely evaluated so far.

Branching enzymes (BEs) are classified into two groups depending on their amino-acid sequences: group I or B-family and group II or A-family (Burton *et al.*, 1995). The *in vitro* determination of catalytic parameters showed that BEI is more active on amylose than amylopectin, in contrast to the members of the BEII group (Guan *et al.*, 1993; Guan *et al.*, 1994). Moreover, BEI transfers longer glucans compared to BEII (Guan *et al.*, 1997). GlgB that generates  $\alpha(1\rightarrow6)$  linkages during glycogen synthesis has catalytic properties obviously distinct to that of maize BEII and BEI (Guan *et al.*, 1997).

In this work, our objective was to test whether the phylogenetic and family origin of BEs was crucial for the production of water-insoluble semi-crystalline polysaccharides. The expression of maize BEI or BEII or both BEI and BEII in a *glgB*- mutant of *E. coli* results in the synthesis of glycogen-like but not starch-like polysaccharides (Guan *et al.*, 1995). Similar results were obtained after the expression of maize BEIIa and/or BEIIb in a branching enzyme mutant of yeast (Seo *et al.*, 2002). Alternatively, *E. coli* glycogen branching enzyme (GlgB) was already expressed in different plants such as potato (Kortstee *et al.*, 1996; Huang *et al.*, 2013) and rice (Kim *et al.*, 2005) leading to modification of the structure of the synthesized polyglucans (increased branching degree

and altered chain length distribution of amylopectin). However in both cases, the endogenous BEs were still active, thus preventing from the determination of the specific contribution of GlgB for the synthesis of starch.

*Arabidopsis* contains only two BEs involved in transitory starch synthesis and both of them belong to the BEII group (Fisher *et al.*, 1996). *Arabidopsis be2 be3* double mutants are unable to create branch points during polysaccharide synthesis and are therefore starchless (Dumez *et al.*, 2006). We used these plants, devoid of endogenous BEs, to express the *E. coli* GlgB glycogen branching enzyme to evaluate whether enzyme metabolic origin (i.e. glycogen versus starch) can sustain the synthesis of starch-like polyglucan, more precisely, a polyglucan that is water-insoluble, partly crystalline, contain both amylopectin and amylose and in which amylopectin DP<sub>max</sub> is 12-13. GlgB is involved in the synthesis of glycogen and belongs to the BEI family (Sawada *et al.*, 2014). The analysis of polyglucan accumulation in *Arabidopsis* plants expressing GlgB revealed that the balance between branching and debranching activities, assuming that elongating activity is not-limiting, establishes the structure of the polysaccharide produced, regardless of the origin of the branching enzyme.

## MATERIALS AND METHODS

### *Cloning of the glycogen branching enzyme (GlgB) of Escherichia coli*

The chloroplast transit peptide of *Arabidopsis thaliana* Branching Enzyme 2 (At5g03650) was identified with the use of ChloroP 1.1 (<http://www.cbs.dtu.dk/services/ChloroP/>). The corresponding nucleotide sequence was

reconstituted by PCR using two long and partially complementary primers, TPbe2-1 and TPbe2-2 (primer sequences and method of amplification are depicted in details in Figure S1). A fragment corresponding to the first 30 nucleotides of the 5' end of *glgB* was then added downstream of the sequence encoding the transit peptide (Figure S1). In parallel, the coding sequence of *glgB* was amplified by PCR from genomic DNA of *E. coli* TOP10 using primers *glgB*-For and *glgB*-Rev (Figure S1). The final sequence was obtained after 20 cycles of polymerase extension of both overlapping sequences. This chimeric cDNA was subsequently amplified by PCR with primers TPbe2 for-CACC and *glgB* rev (Figure S1) and cloned into pENTR™/D-TOPO prior to be transferred by homologous recombination into pMDC32 using the gateway® technology (Life Technologies). The sequence was checked by full-sequencing before further uses. All PCR reactions were performed using a high-fidelity DNA polymerase (Kapa Hifi from KAPABIOSYSTEM®).

#### *Plant transformation and selection*

The *be2 be3* double mutant of *A. thaliana* (WS ecotype) (Dumez *et al.*, 2006) was transformed by the floral dip method using *A. tumefaciens* strain GV3101 (Clough *et al.*, 1998; Jyothishwaran *et al.*, 2007) according to (Facon *et al.*, 2013). Transformed plants were selected for their resistance to hygromycin B. T1 seeds were sterilized according to (Harrison *et al.*, 2006) and sown on petri dishes containing 1% (w/v) Murashige and Skoog medium, 1% (w/v) agar and 20 µg.mL<sup>-1</sup> of hygromycin B (Sigma-Aldrich). Plates were incubated for 2-3 weeks at 22°C, 75% humidity and a specific photoperiod according to (Harrison *et al.*, 2006). 98 hygromycin-resistant individuals were transferred to soil and cultivated in a greenhouse under a 16-h light / 8-h dark photoperiod. The presence of the

transgene was confirmed by PCR amplification of the *glgB* sequence (*glgB*-For and *glgB*-Rev primers) in 22 plants displaying a leaf iodine-staining phenotype (see below) different to that of the *be2 be3* mother plant. A representative panel of eleven plants with different leaf iodine-staining phenotypes was selected and T2 seeds were collected. T2 plants were selected on solid MS medium as described above and 5 homozygous lines were identified by segregation analysis of the hygromycin-resistance trait.

# *Leaf iodine staining*

Approximately 3-week-old leaves were harvested at the end of the day and immediately immersed in 70% hot ethanol. Samples were incubated under shaking at 70°C and ethanol was replaced several times until complete loss of pigments, prior to be rinsed with water and stained by a KI 1% (w/v) - I<sub>2</sub> 0.1% (w/v) solution.

# *Extraction and quantification of polyglucans*

Leaves were harvested at the end of the day, immediately frozen in liquid nitrogen and stored at - 80°C until use. Two different protocols were then applied for polyglucan extraction.

Isolation of insoluble polyglucans (for microscopy and crystallographic analysis) was adapted from (Streb *et al.*, 2008). Several tens of grams of leaves were homogenized in a buffered medium (0.1 M Na-acetate (pH 4.8); 0.05% Triton X-100, 2 mM EDTA) with a blender, and then filtered on two layers of Miracloth (Calbiochem). SDS was added to the filtrate at a final concentration of 1.5% (w/v) and the insoluble polyglucans were collected by centrifugation (20 min at 20,000 g). Then, the samples were washed 4 times with water

and were sequentially filtered on nylon meshes of decreasing pore size, in the order: 100, 31 and 11  $\mu$ m. The filtrates were centrifuged (10 min at 16,000 g) and the polyglucan pellet was resuspended in 20% ethanol and stored at 4°C until use.

Extraction of insoluble and soluble polyglucans (for quantification and ultrastructure analysis) was performed on 1 g of leaves using the perchloric acid method described in detail in (Streb *et al.*, 2008).

The polyglucan content was measured by a spectrophotometric method (Enzytec™, R-BIOPHARM®) following the manufacturer's instructions.

#### *Analysis of the ultrastructure of polyglucans*

The chain length distribution (CLD) of the polyglucans was determined with 200  $\mu$ g of purified material debranched with a mix of 4 U isoamylase (*Pseudomonas sp.*, Megazyme) and 2U pullulanase (*Klebsiella planticola*, Megazyme) in sodium acetate buffer (55 mM final concentration, pH3.5) incubated overnight at 42°C in a final volume of 500  $\mu$ L. After 10 min at 100°C, the mix was desalted on Alltech™ Extract-Clean™ Carbograph columns (Fisher Scientific). First, columns were equilibrated with 5 mL of 25% acetonitrile and washed with 5 mL of deionized sterile water. Then, samples were loaded on the columns and subsequently rinsed with 5ml of deionized water. Sample elution was performed with 2 mL of 25% acetonitrile. The samples were lyophilized and resuspended in 250  $\mu$ L of deionized water. The chain length distribution of each sample was determined by HPAEC-PAD analysis (Dionex® – PA200 CarboPac column) as fully described in (Roussel *et al.*, 2013).

## Starch fractionation

Starch fractionation (separation of high and low mass polymers) was performed by size exclusion chromatography on a Sepharose CL-2B matrix. 1.2 mg of starch was dispersed in 200  $\mu$ L of DMSO (100%) during 15 min at 100 °C. The polymers were precipitated by the addition of 800 $\mu$ L of absolute ethanol. After centrifugation for 5 min at 10,000 g, the pellet was solubilized in 500  $\mu$ L of 10 mM NaOH and loaded onto the column previously equilibrated with 10 mM NaOH (0.5 cm i.d.  $\times$  65 cm) at a flow rate of 12 mL.h<sup>-1</sup>. Fractions of 300  $\mu$ L were collected and the glucans were detected using I<sub>2</sub>/ KI solution (0.1% and 1% w/v respectively).

## Protein extraction

Protein extracts were obtained from approximately 1 g of fresh leaves harvested at the middle of the day and directly frozen in liquid nitrogen. Frozen leaves were finely powdered and immersed in ice-cold 100 mM Tricine/KOH (pH 7.8) 5 mM MgCl<sub>2</sub>, 1 mM DTT containing 0.1 % of protease inhibitor cocktail (ProteaseArrest<sup>TM</sup>, G Biosciences). Samples were centrifuged at 16,000 g at 4°C during 10 min. The supernatant was collected and the protein content was determined by Bradford assay.

## Zymogram of branching enzyme activity

Zymograms of branching enzyme activity were obtained according to the method described by (Tetlow *et al.*, 2004; Tetlow *et al.*, 2008). Branching enzyme activity is detected indirectly by the stimulation of phosphorylase « a ». In the presence of a high

concentration of Glc-1-P and the absence of Pi, phosphorylase « a » synthesizes linear  $\alpha(1\rightarrow4)$ -linked polyglucans that can be branched in  $\alpha(1\rightarrow6)$  if a branching enzyme is in the vicinity. Branching increases the number of available non-reducing ends and thus stimulates phosphorylase « a » polymerizing activity. This leads to the synthesis of branched polyglucans that can be detected in the form of dark brown bands in the gel after iodine staining. In brief, 5% polyacrylamide resolving gel was prepared with 0.2 U.mL<sup>-1</sup> of rabbit phosphorylase « a » (Sigma), 0.1% (w/v) of maltoheptaose (Sigma) and 0.1% (w/v) of acarbose (Sigma-Aldrich). 60 µg of proteins were mixed with loading buffer in a 20:1 ratio (loading buffer: 2 mg.mL<sup>-1</sup> of bromophenol blue and 50% (v/v) glycerol) and loaded onto the gel. After migration (1 h 30 min at 15 V.cm<sup>-1</sup>), the gel was washed twice in 0.4% MES (w/v) and 2.9% sodium citrate (w/v). After incubation for 2 h at 30°C in 0.4% MES (w/v) and 2.9% sodium citrate (w/v) supplemented with 1.4% of glucose-1-phosphate (w/v), 0.09% adenosine monophosphate (w/v), 0.15% EDTA (w/v) and 0.06% DTT (w/v), the gel was revealed with I<sub>2</sub>/KI solution (0.1% / 1% (w/v)).

#### *In vitro assay of branching enzyme activity*

The branching enzyme activity in leaf extracts was determined according to the method described in details by (Tetlow *et al.*, 2008).

#### *Western blotting*

Protein extracts were treated as for zymogram analysis described above. After migration, proteins were transferred to a nitrocellulose membrane (Whatmann) with a transfer buffer (0.025 M Tris; 0.192 M glycine; 20% (v/v) methanol). After transfer the

membrane was incubated in a blocking solution (0.01 M Tris; 0.25 M NaCl, 1.5% (w/v) BSA) during 15 min and then incubated overnight with the primary antibody diluted at 1/5000 in the blocking solution at room temperature. Then the membrane was washed three times in TTBS (0.1 M Tris; 0.25 M NaCl; 0.1% (v/v) Tween 20). The membrane was incubated for 2 h with a 1/30000 dilution of the secondary antibody (anti-rabbit IgG-alkaline phosphatase; Sigma) at room temperature. The membrane was finally rinsed three times with TTBS buffer and developed with the BCIP/NTB substrate kit following manufacturer's instructions (Invitrogen).

The primary antibody raised against GlgB was produced in rabbit by the inoculation of a peptide specific of the *E. coli* branching enzyme (Eurogentec). Peptide sequence: NH<sub>2</sub>-NLYEHSDPREGYHQDW -CONH<sub>2</sub> (position 355-370 of *E. coli* GlgB protein); Protein carrier: KLH.

### *Transmission and scanning electron microscopy*

Strips of freshly cut leaves harvested at the end of the day were fixed with glutaraldehyde, post-fixed with osmium tetroxide and embedded in Epon resin. 70 nm-thin sections were cut with a diamond knife in a Leica UC6 microtome and post-stained with periodic acid thiosemicarbazide silver proteinate (PATAg) (Gallant *et al.*, 1997). Drops of dilute suspensions of purified glucans were deposited on glow-discharged coated copper grids and the preparations were negatively stained with 2% uranyl acetate. All specimens were observed with a Philips CM200 transmission electron microscope (TEM) operating at 80 kV. Images were recorded on Kodak SO163 films. In addition, drops of suspensions of purified glucans were allowed to dry on freshly cleaved mica and coated with Au/Pd. The



specimens were observed with a Jeol JSM6300 scanning electron microscope (SEM) operating at 8 kV and secondary electron images were recorded using the SIS ADDA II system.

### *Wide-angle X-ray scattering*

The crystallinity index of the polyglucan samples was measured by wide-angle X-ray scattering following a method described by (Wattebled *et al.*, 2008).

## **RESULTS**

### *Selection of Arabidopsis lines expressing GlgB*

*glgB* from *E. coli* was fused downstream of the nucleotide sequence encoding AtBE2 (At5g03650) chloroplast transit peptide. The resulting cDNA was then cloned into pMDC32, a binary vector designed for transgene expression under the control of the CaMV 35S promoter. *be2 be3* double mutants were transformed by the floral dip method (Clough *et al.*, 1998) with an *Agrobacterium tumefaciens* strain carrying the construct. Among 6000 plants tested, 98 transformants (T1), displaying hygromycin resistance, were selected on MS agar plates. 5 independent homozygous lines were selected among their progeny (T2 plants) and further analyzed for their leaf iodine-staining phenotype (Figure 1). At the end of the daytime period, while wild-type (WT) leaves stain black due to normal amounts of starch, *be2 be3* leaves stain yellow because they lack polysaccharides. By contrast, *isa1 isa3 pul* leaves stain orange because they accumulate high amounts of phytyglycogen (Wattebled *et al.*, 2008). The phenotypes of the transformants, called “ $\beta$  lines”, were

intermediate between those of WT and *isa1 isa3 pul* lines, suggesting that the polysaccharide synthesis was at least partially restored. However, while  $\beta$ 20 and  $\beta$ 6 lines stain brown,  $\beta$ 12 stains dark brown and  $\beta$ 1 stains dark grey, suggesting different levels of complementation.  $\beta$ 5 is noteworthy since iodine staining is not homogeneous in that line. A grey stain was observed at the apex of some leaves, while other leaves remained yellow. It suggests a non-homogeneous expression of the transgene in that line. For clarity, only  $\beta$ 1,  $\beta$ 12, and  $\beta$ 20 lines, that are representative of each phenotype, will be further presented here. Results obtained for lines  $\beta$ 5 and  $\beta$ 6 are available as Supporting figures (Figure S6; Figure S7 and Figure S8).

The *be2 be3* double mutant displays strong growth retardation probably due to the over-accumulation of maltose (Dumez *et al.*, 2006). Therefore, we analyzed the developmental phenotype of the transformants as well as *be2 be3* and wild-type plants (Figure S2). Contrary to *be2 be3* mutant plants, GlgB-expressing lines were similar to the wild type at maturity.

### ***Expression and activity of GlgB***

The expression of GlgB in the " $\beta$ " lines was confirmed by western blot using a peptide-specific anti-*E. coli* BE antibody raised against a 16-mer peptide of the protein (Figure 2A). As expected, while GlgB is absent in *be2 be3* and WT, a unique band of approximately 85 kDa was observed in the transgenic lines. Interestingly, each of these lines displays increasing band intensity in the order:  $\beta$ 1,  $\beta$ 12 and  $\beta$ 20. Zymograms of BE activity were obtained using cell extracts prepared from leaves harvested at the middle of the light period (Figure 2B). As already described (Dumez *et al.*, 2006), no BE activity is

observed in the *be2 be3* mutant of *Arabidopsis* while WT displays one band of activity on the zymogram (Figure 2B). In contrast, a large activity band of lower mobility was found in the *E. coli* extract. BE electrophoretic profiles of the transgenic lines differ between each other as well as from those of *E. coli* and *Arabidopsis*. Indeed, one band of intermediate mobility (Figure 2B, a + b) is present in all extracts of the three “ $\beta$ ” lines (Figure 2B). Moreover, an additional band with a higher mobility than that of *Arabidopsis* BE is visible in line  $\beta 20$  (Figure 2B, c). Band intensities also vary among “ $\beta$ ” lines, being far greater in  $\beta 12$  and  $\beta 20$  extracts compared to  $\beta 1$  (Figure 2B).

Correlations between zymogram activities and *glgB* expression in the transgenic lines were sought by western blot. Leaf or cell protein extracts were separated by polyacrylamide gel electrophoresis in non-denaturing conditions similar to those used in the zymogram assay. As expected, no cross-reaction could be seen in *Arabidopsis* WT and *be2 be3* samples. One band was observed in the *E. coli* extract, the mobility of which corresponded to the activity detected on the zymogram (Figure 2B and 2C). Similarly, two bands corresponding to the activities observed on the zymogram were visible in the  $\beta 1$ ,  $\beta 12$ , and  $\beta 20$  transgenic lines (Figure 2C, a and b). However, the intensity of the two bands in line  $\beta 1$  was lower than that of the two other transgenic lines. A third band of higher mobility was also clearly visible in line  $\beta 20$  (Figure 2C, c) and may correspond to the high mobility activity observed on the zymogram.

Zymogram and immunoblotting assays suggest that different levels of BE activity can be found in the lines tested in this work. Thus, BE activity was measured *in vitro* by the phosphorylase « a » stimulating assay using  $^{14}\text{C}$ -labeled Glc-1-P (Figure 2D). Leaf extracts were incubated for 10, 20 or 40 min at 30°C and Glc-1-P consumption was plotted against

the incubation time (Figure 2D). This assay confirmed that BE activity increased in the “ $\beta$ ” lines, in the order:  $\beta$ 1,  $\beta$ 12 and  $\beta$ 20. An extremely low level of activity was detected in the *be2 be3* mutant of Arabidopsis (phosphorylase « a » activity is not stimulated because of the lack of BE activity in this line) while WT shows significant incorporation of Glc into polyglucan after 40 min of incubation.

### ***Polyglucan accumulation in the *glgB* expressing lines***

Iodine-staining phenotypes of the transgenic lines expressing *glgB* suggest that starch and/or water-soluble polysaccharide synthesis is at least partially restored despite the lack of endogenous branching enzymes. These polyglucans were assayed after extraction from leaves harvested at the end of the 16-h light period (Figure 3). Wild-type Arabidopsis plants accumulate insoluble polysaccharides and only tiny amounts of non-methanol-precipitable sugars (i.e. glucose and maltooligosaccharides), while methanol-precipitable polysaccharides could not be detected (Figure 3). Interestingly, line  $\beta$ 1 displayed the highest amount of insoluble polyglucans among transgenic lines while it also showed the lowest BE activity (Figure 2 and Figure 3). In line with this, insoluble polysaccharide contents were lower in both  $\beta$ 12 and  $\beta$ 20, in contrast to the levels of BE activity observed in these plants. Interestingly, methanol-precipitable glucans were detected at significant levels in  $\beta$ 12 and  $\beta$ 20 compared to  $\beta$ 1. Finally, non-methanol-precipitable glucans were found at a relatively high level in  $\beta$ 20 (about 1 mg.g<sup>-1</sup> of fresh leaves) compared to the other lines (0.35 mg.g<sup>-1</sup> in  $\beta$ 12; 0.2 mg.g<sup>-1</sup> in  $\beta$ 1; 0.05 mg.g<sup>-1</sup> in WT). Note that in the same culture conditions (16 h light), the *be2 be3* double mutant accumulated very high amounts of maltose (up to 20 mg.g<sup>-1</sup> of fresh weight) (Dumez *et al.*, 2006).

### ***Observation of polyglucans accumulation in leaf chloroplasts***

The accumulation of polyglucans was directly observed *in planta* by transmission electron microscopy (TEM - Figure 4). Ultrathin sections of leaves were observed after positive staining of the polyglucans with PATAg. Flat and smooth starch granules of approximately 1-3  $\mu\text{m}$  were observed in WT (Figure 4A), as already described in the literature. By contrast, no starch granules were detected in the *be2 be3* double mutant, in agreement with the phenotype already described for this line (Figure 4B) (Dumez *et al.*, 2006). The *isa1 isa3 pul* triple mutant was included in this analysis as a starchless phytoglycogen-accumulating line. Phytoglycogen was visible in the form of very small and polydisperse particles homogeneously distributed in the stroma of the chloroplasts (Figure 4C). Different types of particles were observed in the three lines expressing *glgB*. Lines  $\beta 1$  and  $\beta 12$  accumulated 0.2 - 3  $\mu\text{m}$ -large and irregularly shaped particles (Figure 4D and 4E, respectively), while  $\beta 20$  contained significantly smaller and highly polydisperse particles (Figure 4F). The larger objects could reach 1  $\mu\text{m}$  in size but most particles were smaller than 0.2  $\mu\text{m}$ . The image of  $\beta 20$  is thus similar to that of *isa1 isa3 pul* (Figure 4C) although no large aggregates were observed in the images of the triple DBE mutant. The surface of the particles was irregular and rather rough in  $\beta 1$  while it was smoother in  $\beta 12$ . In both specimens, the fact that the larger particles may correspond to the aggregation of smaller units cannot be excluded.

### ***Morphology of purified insoluble and soluble polyglucans***

The insoluble polyglucans were also observed by scanning electron microscopy (SEM) after extraction from leaves and purification (Figure 5). In WT, starch granules appeared as individual flat particles with a smooth surface, as usually observed for Arabidopsis starch granules (Figure 5A). Their size ranged between 1 and 4  $\mu\text{m}$ . The identification of individual particles in extracts from the transgenic lines was very difficult, and aggregates or particle networks were generally observed (Figure 5B-5D). This artefactual aggregation may be due to the repeated centrifugations performed during the polyglucan purification and/or a reconcentration upon drying on the supporting mica. Nevertheless, despite this aggregation, constituting units could be recognized within the particle networks in each image and their size clearly decreased with increasing GlgB activity, in agreement with the TEM observation of ultrathin sections of leaves (Figure 4D-4F).

Higher resolution images of the insoluble polyglucans were recorded by TEM of negatively stained preparations. As the particles extracted from  $\beta 1$  were too large to be observed with this technique, only particles extracted from  $\beta 12$  and  $\beta 20$  are shown in Figure 6. Moreover, only the smallest of these insoluble particles could be properly stained and observed in sufficient detail. Consequently, the images illustrate the morphology of this fraction of particles but may not represent that of the larger objects.

The insoluble polyglucans in  $\beta 12$  often appeared as aggregates of smaller particles with various shape and size (Figure 6A and 6B). 200 nm bulky and rather smooth spheroidal particles could be recognized, often in contact with multilobular less well-defined material. The particles in  $\beta 20$  are more flat and exhibit a clear multilobular aspect

(Figure 6C and 6D). Their average size is still around a few hundreds nanometers but they seem to be composed of 50-70 nm subunits. Although it is difficult to see if the larger particles are aggregates of individual subunits formed upon centrifugation and/or drying, the morphology resembles that of the so-called  $\alpha$ -particles observed in liver glycogen and constituted of smaller  $\beta$ -subunits (Ryu *et al.*, 2009; Sullivan *et al.*, 2012).

TEM images of the polyglucans isolated from the soluble fractions from  $\beta$ 12 and  $\beta$ 20 are shown in Figure 7. In both cases, 20-30 nm particles are observed (Figure 7A and 7B) whose aspect and size distribution are very similar to those of maize phyto glycogen (Figure 7C).

### ***Ultrastructure of insoluble and soluble polyglucans***

The ultrastructure of insoluble and soluble polyglucans was determined and compared to that of reference samples. First, insoluble polyglucans were fractionated by size exclusion chromatography on Sepharose CL-2B<sup>®</sup> (Figure 8). WT starch shows a regular elution profile exhibiting two peaks (Figure 8A). The first peak corresponds to high-mass amylopectin (between 10 and 13 mL) while the second broader peak corresponds to the low-mass amylose (between 16 and 27 mL). The elution profile of insoluble polyglucans for line  $\beta$ 1 also contains two distinct peaks corresponding to high-mass (same elution volume as WT amylopectin) and low-mass material (elution volume equivalent to that of WT amylose), respectively (Figure 8B). However, the peak of low-mass material is much higher and slightly shifted towards lower masses (to the right on the diagram) compared to WT amylose. Moreover, the  $\lambda_{\max}$  of the iodine-polysaccharide complex for high-mass

material in line  $\beta 1$  is 10 nm higher compared to that of WT amylopectin. This suggests that this material is composed, on average, of longer-chain glucans than WT amylopectin.  $\beta 12$  and  $\beta 20$  insoluble polyglucans display more or less the same elution profile (Figure 8C and 8D, respectively). A unique large peak of high-mass material is observed, the elution profile of which is equivalent to that of WT amylopectin. Contrary to WT and  $\beta 1$  insoluble polyglucans, no distinct peak of low-mass material was seen in  $\beta 12$  and  $\beta 20$  lines. In addition, the  $\lambda_{\max}$  of the high-mass material in these two lines was decreased by 10 nm compared to WT amylopectin, suggesting that the length of the glucans is shorter on average (Table1).

The crystallinity index of the insoluble polyglucans was determined by wide-angle X-ray scattering. The analyses were performed on two samples of polyglucans extracted from two plant preparations cultivated independently (Table 1). All samples are of B-type allomorph. The WT starch granules have a crystallinity index of 33%, in agreement with previous reports on Arabidopsis starch (Wattebled *et al.*, 2008). The  $\beta 1$  and  $\beta 12$  insoluble polyglucans display a lower crystallinity index (27 and 20%, respectively), while the  $\beta 20$  insoluble glucans have the lowest crystallinity index (13%) among those analyzed in this work.

The chain length distribution (CLD) profile of the insoluble polyglucans was established after debranching with a mixture of bacterial isoamylase and pullulanase. The resulting linear glucans were separated and quantified by HPAEC-PAD (Figure 9). The profile of  $\beta 1$  polyglucans has a DP max of 12-13 glucosyl residues identical to WT starch (Figure 9A and 9C). However, the fraction of DP 5-18 glucans is higher and the fraction of DP 21-40 is lower in  $\beta 1$  compared to WT. The higher fraction of short glucans (DP<13)



that do not interact with iodine may explain the increase of the  $\lambda_{\max}$  of the iodine-polyglucan complex observed in this sample (Table 1). The  $\beta 12$  insoluble polyglucan has a profile similar to that of  $\beta 1$  although the fraction of DP 5-11 glucans is higher, especially at DP 6-7 (Figure 9A). In  $\beta 20$ , the  $DP_{\max}$  is at DP 7 and the profile strongly resembles that of the insoluble glucan synthesized by the *Arabidopsis isa1 isa3 pul* triple mutant (Figure 9B) apart from a strong depletion of DP 3-4 glucans in  $\beta 20$  that is probably due to the presence of DBE activity in that line compared to the triple DBE mutant.

The branching degree of the insoluble polyglucans was estimated according to the method described in (Szydlowski *et al.*, 2011) (Table 1). WT,  $\beta 1$ ,  $\beta 12$  and  $\beta 20$  polyglucans had branching degrees of 5.1, 6.1, 6.8 and 7.3%, respectively. The branching degree of the phytoglycogen of the *Arabidopsis isa1 isa3 pul* triple mutant was estimated at 8.1%, a value very close to that previously reported (Szydlowski *et al.*, 2011).

The CLD profiles were also established for the soluble polyglucans isolated from the transgenic lines. The corresponding profiles were compared to that of rabbit liver glycogen (Figure S3). In all cases, DP 7 chains were the most abundant among those analyzed. Although the profiles of the transgenic lines were all similar, they were different to that of glycogen with a significant excess of DP 5-13 chains and a deficit in DP > 17 chains.

## DISCUSSION

About 20 years ago, it was suggested that isoamylase-type debranching enzymes (DBEs) were required for the building of the final structure of amylopectin in plants, determining insolubility and partial crystallization (Ball *et al.*, 1996; Mouille *et al.*, 1996; Myers *et al.*, 2000). This idea was further supported and confirmed by several studies

conducted with different plant species (James *et al.*, 1995; Nakamura, 1996; Rahman *et al.*, 1998; Delatte *et al.*, 2005; Wattebled *et al.*, 2005). In all cases, the lack of isoamylase-type DBEs (except the ISA3 isoform dedicated to starch degradation) caused a strong reduction of starch accumulation, and a modification of the ultrastructure of the residual starch accompanied by a decrease of the crystallinity index. Moreover, these isoamylase mutants also accumulate phytyglycogen, a water-soluble and amorphous glucan structure, which is comparable to that of the glycogen found in animals, fungi and bacteria. However, the synthesis of high amounts of insoluble polyglucans was reported in a quintuple mutant of *Arabidopsis* lacking all four DBEs plus one form of plastidial  $\alpha$ -amylase (Streb *et al.*, 2008). Thus, the necessity of DBEs *per se* for the determination of the water-insolubility and crystallinity of starch could be questioned, although the polyglucans synthesized in the above-mentioned quintuple mutant displays specific features (very high DP<10 content for instance) not observed in WT starch. Therefore, the function of branching enzymes (BEs) appears to be crucial in establishing the intrinsic structural features of starch although crystallinity of the polyglucan synthesized in the *Arabidopsis* quintuple mutant was not reported in (Streb *et al.*, 2008). To test this hypothesis, we have substituted *A. thaliana* starch branching enzymes (BE2 and BE3), main contributors to the synthesis of starch in leaves, with the *E. coli* glycogen branching enzyme (GlgB) and the synthesis of polyglucans was investigated. The suppression of both BE2 and BE3 in *Arabidopsis* resulted in the complete loss of starch branching enzyme activity (Figure 2B and 2D) and the loss of starch synthesis and was accompanied by the accumulation of maltose and plant growth retardation (Dumez *et al.*, 2006). Other starch metabolizing enzymes were not affected by the mutations. Thus, the *be2 be3* double mutant represents an excellent model

to investigate the ability of GlgB to restore starch or starch-like polyglucan synthesis in *Arabidopsis*.

The expression of *glgB* in *A. thaliana* was successfully achieved after transformation of the corresponding cDNA into *be2 be3* plants. The corresponding protein was detected by immunoblot analysis of leaf extracts of several independently transformed plants (Figures 2A and 2C) and the branching activity of the enzyme was also detected (Figures 2B and 2D). Different levels of expression were obtained, although all plants analyzed in this study were homozygous for the transgene. Indeed, the level of BE activity was much higher in  $\beta 20$  compared to  $\beta 12$ , and most notably compared to  $\beta 1$  which had the lowest BE activity as measured by zymogram and *in vitro* radioactive assay (Figures 2B and 2D). These levels of activity were correlated with GlgB protein contents. Immunoblot analysis performed under denaturing or non-denaturing conditions (Figures 2A and 2C respectively) showed that the content of GlgB is higher in  $\beta 20$  than in  $\beta 12$  and even more than in  $\beta 1$ , which is in good agreement with the level of activity assayed in each line. Interestingly, immunoblot analysis performed under non-denaturing conditions (Figure 2C) revealed several bands reacting with the anti-GlgB antibody in the transgenic lines. Two major bands (Figure 2B bands a and b) were detected in all three lines and a third band (Figure 2B band c) of higher mobility but lower intensity was specifically observed in  $\beta 20$ . Two additional lines were analyzed during this work:  $\beta 5$  and  $\beta 6$ . Corresponding results are presented as Supporting data in the form of Figures S6, S7 and S8 and confirm the results presented above. Line  $\beta 5$ , which has a very low GlgB activity, displays a phenotype similar to that of  $\beta 1$ . Conversely line  $\beta 6$ , that has high GlgB activity, is similar to  $\beta 20$ . This result

suggests that GlgB is either post-translationally modified when expressed in *Arabidopsis* or is involved in the formation of protein complexes (homo or heteromeric complexes) with different electrophoretic mobility (Tetlow *et al.*, 2004; Makhmoudova *et al.*, 2014).

Although GlgB was expressed and active in all transgenic lines, the phenotype of polyglucan accumulation was different from one line to another. Indeed, albeit displaying the lowest GlgB expression level,  $\beta 1$  accumulated polyglucans with a structure close to that of WT starch. These polyglucans had a granular morphology and individual particles were observed in the stroma of the chloroplast (Figure 4). These granules had a size similar to that of WT starch although their surface appeared to be rougher. Smaller PATAg-stained particles, with a size well below 1  $\mu\text{m}$ , were also dispersed throughout the stroma of  $\beta 1$  chloroplasts. Moreover, the  $\beta 1$  insoluble polyglucan fraction was partially crystalline (27% compared to 33% for WT starch) and was composed of both high-mass amylopectin-like material and low-mass amylose-like material (Figure 8). Further, the CLD profile after debranching was similar to that of WT starch although it was enriched in DP 5-19 chains (with a  $\text{DP}_{\text{max}}$  at 12 glucose residues such as in WT starch) and depleted in DP 21-40 chains (Figure 9). As a whole, the  $\beta 1$  polyglucan can be considered as starch-like implying that a bacterial glycogen BE can sustain the synthesis of such specifically ordered polysaccharide when expressed in plants. It follows that the final distribution of the branch points within starch and consequently the properties of the synthesized polyglucan (crystallinity, water-insolubility, granular morphology, amylopectin  $\text{DP}_{\text{max}}$  at 12-13, and the presence of amylose) is not solely under the control of starch branching enzymes (although branching enzyme activity is mandatory to create  $\alpha(1\rightarrow 6)$  linkages). Otherwise, expression of a

544 bacterial glycogen-branching enzyme in the plant would have resulted in the synthesis of  
545 soluble and amorphous glycogen-like polymers. Nevertheless, the polyglucan that  
546 accumulates in  $\beta 1$  can not be regarded as true WT starch and several hypotheses can be  
547 proposed which could explain why this is the case. Firstly, GlgB is expressed in  
548 *Arabidopsis* under the control of the constitutive 35S promoter. Consequently, GlgB is  
549 likely expressed linearly during the day and the night, which may influence the final  
550 structure of the synthesized polyglucan. However, the expression of the endogenous BEs  
551 (BE2 and BE3) is not strongly correlated with the day/night cycle (Smith *et al.*, 2004).  
552 Indeed, BE2 exhibits only slightly higher expression in the day compared to the night. BE3,  
553 expression is significantly higher during the day compared to night and displays an  
554 expression pattern that resembles that of enzymes involved in starch degradation (Smith *et*  
555 *al.*, 2004), although, more recently, BE3 protein abundance was reported as unmodified  
556 throughout the day/night cycle (Skeffington *et al.*, 2014). The second hypothesis relies to  
557 the intrinsic properties of GlgB activity. Indeed, starch BE isoforms have different catalytic  
558 properties (Tetlow, 2012). In *A. thaliana*, in contrast to other plants and to other dicots,  
559 only class-II branching enzymes (BE2 and BE3) have been described so far. However,  
560 because of its catalytic properties, GlgB can be classified in the class-I plant branching  
561 enzymes and preferentially transfers DP 6-15 chains (with a maximum for DP 10-12  
562 chains) (Guan *et al.*, 1997; Sawada *et al.*, 2014). Therefore it is not surprising that the  
563 expression of a class-I BE instead of class-II BEs results in modifications in the structure of  
564 the synthesized polysaccharide compared to the wild type. Another explanation relates to  
565 enzyme complex formation. It is now well established that some of the starch metabolizing  
566 enzymes interact to form hetero-multimeric complexes (Hennen-Bierwagen *et al.*, 2008;

Tetlow *et al.*, 2008; Hennen-Bierwagen *et al.*, 2009). Branching enzymes are important components of these complexes as shown in the endosperm of cereals (Liu *et al.*, 2009; Liu *et al.*, 2012a; Liu *et al.*, 2012b). Although it has not been shown yet, it is likely that starch-metabolizing enzymes also organize in the form of multisubunit complexes in Arabidopsis. It is highly probable that BE2/BE3 and GlgB are engaged in different protein complexes or simply that GlgB is unable to interact with other endogenous plant enzymes. This could result in the modification of other starch-metabolizing activities and consequently polyglucan structure. Even if enzymes of starch synthesis do not physically interact in Arabidopsis chloroplasts, their activities must still be interdependent in order to produce the final structure of amylopectin. Removing one or several enzymes of the pathway could alter the activity of others whose normal activity depends on the presence of the complete set of enzymes (Szydlowski *et al.*, 2011; Nakamura *et al.*, 2012; Abe *et al.*, 2014; Brust *et al.*, 2014; Nakamura *et al.*, 2014). GlgB may only partially counterbalance the lack of both BE2 and BE3 in the transgenic lines, which, in turn, may alter other starch-metabolizing activities. Lastly, some starch-metabolizing enzymes are regulated by the redox state of the cell or the organelle where the pathway occurs (Glaring *et al.*, 2012; Lepisto *et al.*, 2013). It is possible that GlgB does not behave like Arabidopsis BEs which are redox sensitive (Glaring *et al.*, 2012), thus modifying the branching activity in the transgenic lines and explaining why it is not possible to restore a true WT phenotype.

Finally, it should be emphasized that the ability to form starch-like structures depends on the level of branching enzyme activity of GlgB. Indeed,  $\beta 20$ , which possessed the highest GlgB activity, synthesizes polyglucans whose structure resembles more or less

that of the residual insoluble glucans isolated from *Arabidopsis* DBE mutants (Wattebled *et al.*, 2008). The  $\beta 12$  line, that had a GlgB activity intermediate between that of  $\beta 1$  and  $\beta 20$ , displays an intermediate polyglucan-accumulating phenotype. Debranching enzyme activity level was estimated in the different lines by zymogram analysis (Figure S4). No obvious modification of isoamylase activity was detected in the GlgB-expressing plants compared to the wild type. Starch synthase activity was also evaluated with zymograms (Figure S5). SS1 and SS3 are the two major isoforms of starch synthases encompassing over 90% of the elongating activity measured in *Arabidopsis* leaf extracts (Szydlowski *et al.*, 2011). Starch synthase activities were unmodified in the *be2 be3* mutant (Dumez *et al.*, 2006). Both SS1 and SS3 activities were reduced in  $\beta 1$  compared to WT. The activity of SS1 was slightly higher in  $\beta 12$  and  $\beta 20$  compared to WT whereas SS3 was, to some extent, reduced. At this stage it is unclear why starch synthase activity is modified in the transgenic lines, especially in  $\beta 1$ . Nevertheless, despite possessing the lowest starch synthase activity,  $\beta 1$  is the GlgB expressing line accumulating the highest amount of insoluble polyglucans. Thus the remaining SS activity in  $\beta 1$  appears to be in excess of that needed to allow the synthesis of the insoluble polyglucan, and does not seem to be a limiting factor.

Thus, in a context of non-limiting starch synthase activity, the accumulation of the insoluble and soluble polyglucans in  $\beta 20$  occurs under circumstances of over-branching which cannot be balanced by the debranching activity of endogenous isoamylases and pullulanase. This results in a higher branching degree (7.3%) and a very low crystallinity index (13%) of the insoluble polyglucans in  $\beta 20$ . Such increase of the branching degree of the polyglucan produced in plants after the expression of *E. coli* GlgB has already been

described in potato and rice (Kortstee *et al.*, 1996; Kim *et al.*, 2005). In both cases, the number of branch points of amylopectin was significantly increased. However, because endogenous BE activity was not knocked down in these plants the actual contribution of GlgB for the synthesis of the highly branched starch was impossible to determine.

Our result suggests that a finely tuned balance between branching and debranching activities is probably acting *in planta* to control  $\alpha(1\rightarrow6)$  linkage placement and number, and consequently to allow the formation of starch or starch-like polyglucan. Figure 10 is an attempt to model our interpretation of the results generated in this work. As a model, it is likely a simplified view of reality (for instance starch synthases are not included in the model) and was conceptualized from the results of the expression of a bacterial enzyme in plants. However, we suggest that it could be generalized to any situation where the balance between BE and DBE activity is compromised. For instance, in rice, the endogenous BEIIb isoform was expressed in a BEIIb-defective mutant by expression of the corresponding structural gene (Tanaka *et al.*, 2004). Overexpression of the protein and of the corresponding activity was obtained in one of the transgenic lines leading to the accumulation of significantly higher amount of soluble polyglucan compared to the wild type (almost three times more). This was accompanied by enrichment in DP<15 glucans of amylopectin and alteration of the crystalline structure of starch.

Nevertheless expression of GlgB did not restore the synthesis of true WT starch, possibly because GlgB activity cannot be regulated in the same way as endogenous BEs. Protein complexes and thus other enzyme activities (starch synthases for instance) might be



632 affected by the lack of endogenous BEs, leading to the synthesis of structurally modified  
633 polyglucan as frequently observed in mutants defective for enzymes of the pathway.

## 634    **ACKNOWLEDGEMENTS**

635            The authors thank Dr. Nicolas Szydlowski for fruitful discussions and critical  
636    reading of the manuscript, and gratefully acknowledge the financial support of Agence  
637    Nationale de la Recherche (contract # ANR-11-BSV6-0003) and the Natural Sciences and  
638    Engineering Research Council of Canada (Team Discovery Grant, number 435781, MJE,  
639    IJT).

## REFERENCES

- Abe N., Asai H., Yago H., Oitome N., Itoh R., Crofts N., . . . Fujita N. (2014) Relationships between starch synthase I and branching enzyme isozymes determined using double mutant rice lines. *BMC Plant Biology*, **14**, 80.
- Ball S., Guan H.-P., James M., Myers A., Keeling P., Mouille G., . . . Preiss J. (1996) From Glycogen to Amylopectin: A Model for the Biogenesis of the Plant Starch Granule. *Cell*, **86**, 349-352.
- Ball S.G. & Morell M.K. (2003) From bacterial glycogen to starch: understanding the biogenesis of the plant starch granule. *Annu Rev Plant Biol*, **54**, 207-233.
- Bertoft E. (2004) On the nature of categories of chains in amylopectin and their connection to the super helix model. *Carbohydrate Polymers*, **57**, 211-224.
- Bertoft E. (2013) On the building block and backbone concepts of amylopectin structure. *Cereal Chemistry*, **90**, 294-311.
- Brust H., Lehmann T., D'Hulst C. & Fettke J. (2014) Analysis of the functional interaction of Arabidopsis starch synthase and branching enzyme isoforms reveals that the cooperative action of SSI and BEs results in glucans with polymodal chain length distribution similar to amylopectin. *PLoS One*, **9**, e102364.
- Buleon A., Colonna P., Planchot V. & Ball S. (1998) Starch granules: structure and biosynthesis. *International Journal of Biological Macromolecules*, **23**, 85-112.

660 Burton R.A., Bewley J.D., Smith A.M., Bhattacharyya M.K., Tatge H., Ring S., . . . Martin  
661 C. (1995) Starch branching enzymes belonging to distinct enzyme families are  
662 differentially expressed during pea embryo development. *Plant J*, **7**, 3-15.

663 Clough S.J. & Bent A.F. (1998) Floral dip: a simplified method for *Agrobacterium*-  
664 mediated transformation of *Arabidopsis thaliana*. *Plant J*, **16**, 735-743.

665 Delatte T., Trevisan M., Parker M.L. & Zeeman S.C. (2005) *Arabidopsis* mutants *Atisa1*  
666 and *Atisa2* have identical phenotypes and lack the same multimeric isoamylase,  
667 which influences the branch point distribution of amylopectin during starch  
668 synthesis. *Plant J*, **41**, 815-830.

669 Dumez S., Wattebled F., Dauvillée D., Delvallé D., Planchot V., Ball S.G. & D'Hulst C.  
670 (2006) Mutants of *Arabidopsis* lacking starch branching enzyme II substitute  
671 plastidial starch synthesis by cytoplasmic maltose accumulation. *Plant Cell*, **18**,  
672 2694-2709.

673 Facon M., Lin Q., Azzaz A.M., Hennen-Bierwagen T.A., Myers A.M., Putaux J.L., . . .  
674 Wattebled F. (2013) Distinct functional properties of isoamylase-type starch  
675 debranching enzymes in monocot and dicot leaves. *Plant Physiol*, **163**, 1363-1375.

676 Fisher D.K., Gao M., Kim K.N., Boyer C.D. & Guiltinan M.J. (1996) Two closely related  
677 cDNAs encoding starch branching enzyme from *Arabidopsis thaliana*. *Plant Mol*  
678 *Biol*, **30**, 97-108.

679 Fujita N. & Nakamura Y. (2012) Distinct and overlapping functions of starch synthase  
680 isoforms. In: *Starch: Origins, Structure and Metabolism*. (ed I.J. Tetlow), pp. 115-  
681 140. Society for Experimental Biology, London, UK.

682 Gallant D.J., Bouchet B. & Baldwin P.M. (1997) Microscopy of starch: evidence of a new  
683 level of granule organization. *Carbohydrate Polymers*, **32**, 177-191.

684 Glaring M.A., Skryhan K., Kotting O., Zeeman S.C. & Blennow A. (2012) Comprehensive  
685 survey of redox sensitive starch metabolising enzymes in *Arabidopsis thaliana*.  
686 *Plant Physiol Biochem*, **58**, 89-97.

687 Guan H., Kuriki T., Sivak M. & Preiss J. (1995) Maize branching enzyme catalyzes  
688 synthesis of glycogen-like polysaccharide in glgB-deficient *Escherichia coli*. *Proc*  
689 *Natl Acad Sci U S A*, **92**, 964-967.

690 Guan H., Li P., Imparl-Radosevich J., Preiss J. & Keeling P. (1997) Comparing the  
691 Properties of *Escherichia coli* Branching Enzyme and Maize Branching Enzyme.  
692 *Archives of Biochemistry and Biophysics*, **342**, 92-98.

693 Guan H.P., Baba T. & Preiss J. (1994) Expression of branching enzyme I of maize  
694 endosperm in *Escherichia coli*. *Plant Physiol.*, **104**, 1449-1453.

695 Guan H.P. & Preiss J. (1993) Differentiation of the properties of the branching isozymes  
696 from maize (*Zea mays*). *Plant Physiol*, **102**, 1269-1273.

697 Harrison S.J., Mott E.K., Parsley K., Aspinall S., Gray J.C. & Cottage A. (2006) A rapid  
698 and robust method of identifying transformed *Arabidopsis thaliana* seedlings  
699 following floral dip transformation. *Plant Methods*, **2**, 19.

700 Hennen-Bierwagen T.A., Lin Q., Grimaud F., Planchot V., Keeling P.L., James M.G. &  
701 Myers A.M. (2009) Proteins from multiple metabolic pathways associate with  
702 starch biosynthetic enzymes in high molecular weight complexes: a model for  
703 regulation of carbon allocation in maize amyloplasts. *Plant Physiol*, **149**, 1541-  
704 1559.

Hennen-Bierwagen T.A., Liu F., Marsh R.S., Kim S., Gan Q., Tetlow I.J., . . . Myers A.M. (2008) Starch biosynthetic enzymes from developing maize endosperm associate in multisubunit complexes. *Plant Physiol*, **146**, 1892-1908.

Hizukuri S. (1986) Polymodal distribution of the chain lengths of amylopectins, and its significance. *Carbohydrate Research*, **147**, 342-347.

Huang X.-F., Nazarian-Firouzabadi F., Vincken J.-P., Ji Q., Suurs L.C.J.M., Visser R.G.F. & Trindade L.M. (2013) Expression of an engineered granule-bound *Escherichia coli* glycogen branching enzyme in potato results in severe morphological changes in starch granules. *Plant Biotechnology Journal*, **11**, 470-479.

James M.G., Robertson D.S. & Myers A.M. (1995) Characterization of the maize gene *sugary1*, a determinant of starch composition in kernels. *Plant Cell*, **7**, 417-429.

Jyothishwaran G., Kotresha D., Selvaraj T., Srideshikan S.M., Rajvanshi P.K. & Jayabaskaran C. (2007) A modified freeze-thaw method for efficient transformation of *Agrobacterium tumefaciens*. *Current Science*, **93**, 770-772.

Kim W.S., Kim J., Krishnan H.B. & Nahm B.H. (2005) Expression of *Escherichia coli* branching enzyme in caryopses of transgenic rice results in amylopectin with an increased degree of branching. *Planta*, **220**, 689-695.

Kortstee A.J., Vermeesch A.M., de Vries B.J., Jacobsen E. & Visser R.G. (1996) Expression of *Escherichia coli* branching enzyme in tubers of amylose-free transgenic potato leads to an increased branching degree of the amylopectin. *Plant J*, **10**, 83-90.

Lepisto A., Pakula E., Toivola J., Krieger-Liszkay A., Vignols F. & Rintamaki E. (2013) Deletion of chloroplast NADPH-dependent thioredoxin reductase results in inability

728 to regulate starch synthesis and causes stunted growth under short-day  
729 photoperiods. *J Exp Bot*, **64**, 3843-3854.

730 Liu F., Ahmed Z., Lee E.A., Donner E., Liu Q., Ahmed R., . . . Tetlow I.J. (2012a) Allelic  
731 variants of the amylose extender mutation of maize demonstrate phenotypic  
732 variation in starch structure resulting from modified protein-protein interactions. *J*  
733 *Exp Bot*, **63**, 1167-1183.

734 Liu F., Makhmoudova A., Lee E.A., Wait R., Emes M.J. & Tetlow I.J. (2009) The amylose  
735 extender mutant of maize conditions novel protein-protein interactions between  
736 starch biosynthetic enzymes in amyloplasts. *J Exp Bot*, **60**, 4423-4440.

737 Liu F., Romanova N., Lee E.A., Ahmed R., Evans M., Gilbert E.P., . . . Tetlow I.J. (2012b)  
738 Glucan affinity of starch synthase IIa determines binding of starch synthase I and  
739 starch-branching enzyme IIb to starch granules. *Biochem J*, **448**, 373-387.

740 Makhmoudova A., Williams D., Brewer D., Massey S., Patterson J., Silva A., . . . Emes  
741 M.J. (2014) Identification of multiple phosphorylation sites on maize endosperm  
742 starch branching enzyme IIb, a key enzyme in amylopectin biosynthesis. *J Biol*  
743 *Chem*, **289**, 9233-9246.

744 Melendez-Hevia E., Waddell T.G. & Shelton E.D. (1993) Optimization of molecular design  
745 in the evolution of metabolism: the glycogen molecule. *Biochem J*, **295 ( Pt 2)**, 477-  
746 483.

747 Mouille G., Maddelein M.L., Libessart N., Talaga P., Decq A., Delrue B. & Ball S. (1996)  
748 Preamylopectin processing: a mandatory step for starch biosynthesis in plants. *Plant*  
749 *Cell*, **8**, 1353-1366.

750 Myers A.M., Morell M.K., James M.G. & Ball S.G. (2000) Recent progress toward  
751 understanding biosynthesis of the amylopectin crystal. *Plant Physiol*, **122**, 989-997.

752 Nakamura Y. (1996) Some properties of starch debranching enzymes and their possible  
753 role in amylopectin biosynthesis. *Plant Science*, **121**, 1-18.

754 Nakamura Y., Aihara S., Crofts N., Sawada T. & Fujita N. (2014) In vitro studies of  
755 enzymatic properties of starch synthases and interactions between starch synthase I  
756 and starch branching enzymes from rice. *Plant Sci*, **224**, 1-8.

757 Nakamura Y., Ono M., Utsumi C. & Steup M. (2012) Functional interaction between  
758 plastidial starch phosphorylase and starch branching enzymes from rice during the  
759 synthesis of branched maltodextrins. *Plant Cell Physiol*, **53**, 869-878.

760 Pfister B., Lu K.J., Eicke S., Feil R., Lunn J.E., Streb S. & Zeeman S.C. (2014) Genetic  
761 evidence that chain length and branch point distributions are linked determinants of  
762 starch granule formation in Arabidopsis. *Plant Physiol*, **165**, 1457-1474.

763 Rahman A., Wong K., Jane J., Myers A.M. & James M.G. (1998) Characterization of SU1  
764 isoamylase, a determinant of storage starch structure in maize. *Plant Physiol*, **117**,  
765 425-435.

766 Roach P.J., Depaoli-Roach A.A., Hurley T.D. & Tagliabracci V.S. (2012) Glycogen and its  
767 metabolism: some new developments and old themes. *Biochem J*, **441**, 763-787.

768 Roussel X., Lancelon-Pin C., Vikso-Nielsen A., Rolland-Sabate A., Grimaud F., Potocki-  
769 Veronese G., . . . D'Hulst C. (2013) Characterization of substrate and product  
770 specificity of the purified recombinant glycogen branching enzyme of  
771 *Rhodothermus obamensis*. *Biochim Biophys Acta*, **1830**, 2167-2177.



772 Ryu J.H., Drain J., Kim J.H., McGee S., Gray-Weale A., Waddington L., . . . Stapleton D.  
773 (2009) Comparative structural analyses of purified glycogen particles from rat liver,  
774 human skeletal muscle and commercial preparations. *Int J Biol Macromol*, **45**, 478-  
775 482.

776 Satoh H., Nishi A., Yamashita K., Takemoto Y., Tanaka Y., Hosaka Y., . . . Nakamura Y.  
777 (2003) Starch-Branching Enzyme I-Deficient Mutation Specifically Affects the  
778 Structure and Properties of Starch in Rice Endosperm. *Plant Physiol.*, **133**, 1111-  
779 1121.

780 Sawada T., Nakamura Y., Ohdan T., Saitoh A., Francisco P.B., Jr., Suzuki E., . . . Ball S.  
781 (2014) Diversity of reaction characteristics of glucan branching enzymes and the  
782 fine structure of alpha-glucan from various sources. *Arch Biochem Biophys*, **562**, 9-  
783 21.

784 Schwall G.P., Safford R., Westcott R.J., Jeffcoat R., Tayal A., Shi Y.-C., . . . Jobling S.A.  
785 (2000) Production of very-high-amylose potato starch by inhibition of SBE A and  
786 B. *Nat Biotech*, **18**, 551-554.

787 Seo B.S., Kim S., Scott M.P., Singletary G.W., Wong K.S., James M.G. & Myers A.M.  
788 (2002) Functional interactions between heterologously expressed starch-branching  
789 enzymes of maize and the glycogen synthases of Brewer's yeast. *Plant Physiol*, **128**,  
790 1189-1199.

791 Skeffington A.W., Graf A., Duxbury Z., Gruissem W. & Smith A.M. (2014) Glucan, Water  
792 Dikinase Exerts Little Control over Starch Degradation in Arabidopsis Leaves at  
793 Night. *Plant Physiology*, **165**, 866-879.

794 Smith S.M., Fulton D.C., Chia T., Thorneycroft D., Chapple A., Dunstan H., . . . Smith  
795 A.M. (2004) Diurnal Changes in the Transcriptome Encoding Enzymes of Starch  
796 Metabolism Provide Evidence for Both Transcriptional and Posttranscriptional  
797 Regulation of Starch Metabolism in Arabidopsis Leaves. *Plant Physiol.*, **136**, 2687-  
798 2699.

799 Streb S., Delatte T., Umhang M., Eicke S., Schorderet M., Reinhardt D. & Zeeman S.C.  
800 (2008) Starch granule biosynthesis in Arabidopsis is abolished by removal of all  
801 debranching enzymes but restored by the subsequent removal of an endoamylase.  
802 *Plant Cell*, **20**, 3448-3466.

803 Sullivan M.A., O'Connor M.J., Umana F., Roura E., Jack K., Stapleton D.I. & Gilbert R.G.  
804 (2012) Molecular insights into glycogen alpha-particle formation.  
805 *Biomacromolecules*, **13**, 3805-3813.

806 Szydlowski N., Ragel P., Hennen-Bierwagen T.A., Planchot V., Myers A.M., Merida A., . .  
807 . Wattebled F. (2011) Integrated functions among multiple starch synthases  
808 determine both amylopectin chain length and branch linkage location in Arabidopsis  
809 leaf starch. *J Exp Bot*, **62**, 4547-4559.

810 Tanaka N., Fujita N., Nishi A., Satoh H., Hosaka Y., Ugaki M., . . . Nakamura Y. (2004)  
811 The structure of starch can be manipulated by changing the expression levels of  
812 starch branching enzyme IIb in rice endosperm. *Plant Biotechnology Journal*, **2**,  
813 507-516.

814 Tetlow I.J. (2012) Branching enzymes and their role in determining structural and  
815 functional properties of polyglucans. In: *Starch: Origins, Structure and Metabolism*.  
816 (ed I.J. Tetlow), pp. 141-178. Society for Experimental Biology, London, UK.

817 Tetlow I.J., Beisel K.G., Cameron S., Makhmoudova A., Liu F., Bresolin N.S., . . . Emes  
818 M.J. (2008) Analysis of protein complexes in wheat amyloplasts reveals functional  
819 interactions among starch biosynthetic enzymes. *Plant Physiol*, **146**, 1878-1891.

820 Tetlow I.J., Wait R., Lu Z., Akkasaeng R., Bowsher C.G., Esposito S., . . . Emes M.J.  
821 (2004) Protein phosphorylation in amyloplasts regulates starch branching enzyme  
822 activity and protein-protein interactions. *Plant Cell*, **16**, 694-708.

823 Wattebled F., Dong Y., Dumez S., Delvalle D., Planchot V., Berbezy P., . . . D'Hulst C.  
824 (2005) Mutants of Arabidopsis lacking a chloroplastic isoamylase accumulate  
825 phytoglycogen and an abnormal form of amylopectin. *Plant Physiol*, **138**, 184-195.

826 Wattebled F., Planchot V., Dong Y., Szydlowski N., Pontoire B., Devin A., . . . D'Hulst C.  
827 (2008) Further evidence for the mandatory nature of polysaccharide debranching for  
828 the aggregation of semicrystalline starch and for overlapping functions of  
829 debranching enzymes in Arabidopsis leaves. *Plant Physiol*, **148**, 1309-1323.

830 Yao Y., Thompson D.B. & Guiltinan M.J. (2004) Maize Starch-Branching Enzyme  
831 Isoforms and Amylopectin Structure. In the Absence of Starch-Branching Enzyme  
832 IIb, the Further Absence of Starch-Branching Enzyme Ia Leads to Increased  
833 Branching. *Plant Physiol.*, **136**, 3515-3523.

834

## TABLES

**Table 1:** The branching degree was calculated according to (Szydlowski *et al.*, 2011). The  $\lambda_{\max}$  of the iodine-amylopectin complex was determined after insoluble polyglucans fractionation by SEC on CL-2B matrix (Figure 8). It was determined at the fraction of maximum absorbance. The crystallinity index and allomorph were determined by wide-angle X-ray scattering. All samples were of B-type. The values are the means of two independent assays. In the case of the *isa1 isa3 pul* triple mutant, the branching degree was determined for phytoglycogen. NA = not available.

Sample	WT	$\beta 1$	$\beta 12$	$\beta 20$	<i>isa1 isa3 pul</i>
Branching degree (%)	5.1	6.1	6.8	7.3	8.1
$\lambda_{\max}$ of amylopectin (nm)	563	572	553	552	NA
Crystallinity index (%)	33	27	20	13	NA

## FIGURE LEGENDS

**Figure 1: Iodine staining of individual plants harvested at the end of the day.** 2-week old plants were harvested and stained with iodine solution after being destained in hot ethanol. All pictures are at the same scale. Colors and intensity of the stain is indicative of the polyglucan content and structure. Wild-type (WT) plants stain dark brown because of the synthesis of high amount of normal starch (ecotype *Wassilewskija*). The *be2 be3* plants stain yellow as a consequence of the lack of any polyglucan in this mutant (Dumez *et al.*, 2006). *isa1 isa3 pul* is a debranching enzyme triple mutant accumulating high amount of phytoglycogen (Wattebled *et al.*, 2008) and therefore stains orange with iodine.  $\beta 1$ ,  $\beta 5$ ,  $\beta 6$ ,  $\beta 12$  and  $\beta 20$  are hygromycin resistant plants selected after transformation of the *be2 be3* mutant with a vector containing the *E. coli glgB* gene. Intermediate colors between those of the WT and the *isa1 isa2* mutant were obtained suggesting that polyglucan synthesis is partially restored in these transgenic lines.

**Figure 2: Expression of glgB in the *be2 be3* transformed lines.** (A) Immunoblot analysis performed in denaturing conditions. Protein extracts were denatured before and during migration in the polyacrylamide gel. After migration, proteins were blotted onto a nitrocellulose membrane and hybridized with a peptide-directed antibody raised against GlgB. (B) zymogram of branching enzyme activity. The polyacrylamide gel contains DP7 maltooligosaccharides and phosphorylase “a”. Branching enzyme activity was revealed by incubating the gel for 2 hours in a phosphorylase “a” stimulating buffer. Bands of branched polyglucans were detected by soaking the gel in iodine solution. (C) Immunoblot analysis performed in non-denaturing conditions: protein extract preparation and migration in the

gel was carried out as in (B). After migration, proteins were treated as in (A). WT: wild type of *A. thaliana* (*Wassilewskija* ecotype);  $\beta 1$ ,  $\beta 12$ ,  $\beta 20$ : transgenic plants expressing GlgB; *be2 be3*: branching enzyme double mutant (Dumez *et al.*, 2006); *E. coli*: bacterial cell extract of wild type *E. coli*. Proteins or activity bands corresponding to GlgB expressed in plants were labelled as a, b, and c. In (A), (B) and (C) all lines are from the same gel and blots. (D) *in vitro* assay of branching enzyme activity. Protein extracts were incubated for 10 to 40 min in a buffer containing DP7 maltooligosaccharides, phosphorylase “a” and [U- $^{14}\text{C}$ ]Glc-1-P (7.4 kBq per assay) at 50 mM final concentration. The mean of incorporated Glc into branched polyglucans was calculated for 3 independent assays and plotted against the time of incubation. Vertical lines stand for standard deviation. Open diamonds: WT extract; closed squares: *be2 be3* mutant; closed circles:  $\beta 1$ ; open squares:  $\beta 12$ ; open circles:  $\beta 20$ .

**Figure 3: Leaf glucan contents.** Glucans were extracted from leaves of 3-week old plants by the perchloric acid protocol. Leaves were harvested at the end of 16-h light period. Insoluble and soluble polyglucans and sugars/maltooligosaccharides were assayed by a spectrophotometric method. The averages of three independent cultures are presented. WT: wild type *WS* ecotype;  $\beta 1$ ,  $\beta 12$ ,  $\beta 20$ : transgenic plants expressing the *E. coli glgB* gene. Vertical thin bars are the standard deviation of three independent biological replicates.

**Figure 4: Transmission electron microscopy of leaf chloroplasts.** Leaves from plants were harvested at the end of the day, cut in small strips and immediately fixed with glutaraldehyde in a cacodylate buffer and stained with PATAg to reveal glucans. A: wild

type from *Wassilewskija* ecotype of *A. thaliana*; B: *be2 be3*: branching enzyme double mutant; C: *isa1 isa3 pul1*: debranching enzyme triple mutant accumulating phyto glycogen (Wattebled *et al.*, 2008); D:  $\beta 1$ , E:  $\beta 12$ , F:  $\beta 20$ : *be2 be3* transgenic plants expressing the bacterial *glgB* gene.

**Figure 5: Scanning electron microscopy of purified insoluble polyglucans.** Insoluble polyglucans were extracted and purified from leaves of 3-week-old plants harvested at the end of the day of 16-h light / 8-h dark cycles. A: wild type *Wassilewskija* ecotype; B:  $\beta 1$ ; C:  $\beta 12$ ; D:  $\beta 20$ .

**Figure 6: Morphology of particles purified from the insoluble polyglucans of the GlgB-expressing lines.** TEM images of negatively stained particles from the insoluble fractions of  $\beta 12$  (A, B) and  $\beta 20$  (C, D).

**Figure 7: Morphology of particles purified from the soluble polyglucans isolated from the GlgB-expressing lines.** TEM images of negatively stained particles from the water-soluble polyglucans isolated from  $\beta 12$  (A) and  $\beta 20$  (B). The image of maize phytoglycogen (C) is given for comparison.

**Figure 8: Fractionation of insoluble polyglucans by size exclusion chromatography.** Purified insoluble polyglucans were dispersed in DMSO, solubilized in NaOH 10 mM and loaded onto a Sepharose® CL-2B matrix. Elution was conducted in NaOH 10 mM at a rate of 12 mL.h<sup>-1</sup>. 300  $\mu$ L fractions were collected and subsequently analyzed by iodine spectrophotometry. Thick continuous lines are the maximum absorbance of the iodine-polyglucan complexes (left Y-axis). Dashed lines indicate the

wavelength (nm) of the iodine-polyglucan complex at the maximum of absorbance (right Y-axis). X-axis is the volume of elution in mL. A: WT; B:  $\beta$ 1; C:  $\beta$ 12; D:  $\beta$ 20.

**Figure 9: Chain length distribution of insoluble polyglucans.** Purified insoluble polyglucans were digested with a mix of bacterial debranching enzymes. The corresponding linear glucans were separated by high-performance anion exchange chromatography and detected by pulsed amperometric detection (HPAEC-PAD). The fraction of each DP (from 3 to 60 glucose residues) is expressed in % of the total DP presented on the profile. (A) WT: continuous black line;  $\beta$ 1: grey triangles;  $\beta$ 12: closed circles;  $\beta$ 20: discontinuous grey line. (B) Comparison of the profiles of the WT (continuous black line) and  $\beta$ 20 (discontinuous grey line). The profile of the *isa1 isa3 pul* triple mutant already published in (Wattebled *et al.*, 2008) is given (open diamonds). (C) Comparison of the profiles of the WT (continuous black line) and  $\beta$ 1 (grey triangles).

**Figure 10: Starch or starch-like polyglucan synthesis occurs thanks to a balanced branching / debranching activity ratio assuming that starch synthase activity is not limiting whatever the branching/debranching ratio.** Left panel: in the absence of branching activity (*be2 be3* double mutant), starch or phytoglycogen synthesis is impossible and is substituted by maltose accumulation; the BR/DEBR ratio is null. Middle panel: when the ratio BR/DEBR activity is balanced (WT) or near-balanced ( $\beta$ 1), starch or starch-like polyglucan synthesis is promoted. In the case of  $\beta$ 1, the slight structural modification of starch is due to the expression of the bacterial glycogen-branching enzyme that has different catalytic and regulatory properties. Right panel: in the absence of debranching activity (such as in *isa1 isa3 pul*; BR/DEBR is infinite) or when branching



932 activity is extremely high (such as in  $\beta$ 20; BR/DEBR >> optimal) phytoglycogen or  
 933 phytoglycogen-like insoluble polyglucan is synthesized respectively. Superimposed  
 934 drawings correspond to (from left to right): maltose, amylopectin, phytoglycogen; black  
 935 points depict the reducing end.

936

## 937     **SUPPORTING INFORMATION**

938     Supporting Figure S1: **Description of the approach employed for the synthesis the GlgB**  
 939     **chimeric sequence used for expression in *A. thaliana*.**

940     Supporting Figure S2: **Comparison of mature plant size.**

941     Supporting Figure S3: **Chain length distribution profiles of water-soluble polyglucans.**

942     Supporting Figure S4: **Zymogram analysis of starch and  $\beta$ -limit dextrins hydrolyzing**  
 943     **enzymes from transformed plants expressing GlgB.**

944     Supporting Figure S5: **Zymogram analysis of soluble starch synthases activities.**

945     Supporting Figure S6: **Expression of GlgB in the *be2 be3* transformed lines.**

946     Supporting Figure S7: **Structure of polysaccharides produced in  $\beta 5$  and  $\beta 6$**   
 947     **transformant lines.**

948     Supporting Figure S8: **Leaf glucan contents and granules morphology.**



**Figure 1: Iodine staining of individual plants harvested at the end of the day.** 2-week old plants were harvested and stained with iodine solution after being destained in hot ethanol. All pictures are at the same scale. Colors and intensity of the stain is indicative of the polyglucan content and structure. Wild-type (WT) plants stain dark brown because of the synthesis of high amount of normal starch (ecotype *Wassilewskija*). The *be2 be3* plants stain yellow as a consequence of the lack of any polyglucan in this mutant ([Dumez et al. 2006](#)). *isa1 isa3 pu1* is a debranching enzyme triple mutant accumulating high amount of phytoglycogen ([Wattebled et al. 2008](#)) and therefore stains orange with iodine.  $\beta 1$ ,  $\beta 5$ ,  $\beta 6$ ,  $\beta 12$  and  $\beta 20$  are hygromycin resistant plants selected after transformation of the *be2 be3* mutant with a vector containing the *E. coli glgB* gene. Intermediate colors between those of the WT and the *isa1 isa2* mutant were obtained suggesting that polyglucan synthesis is partially restored in these transgenic lines.

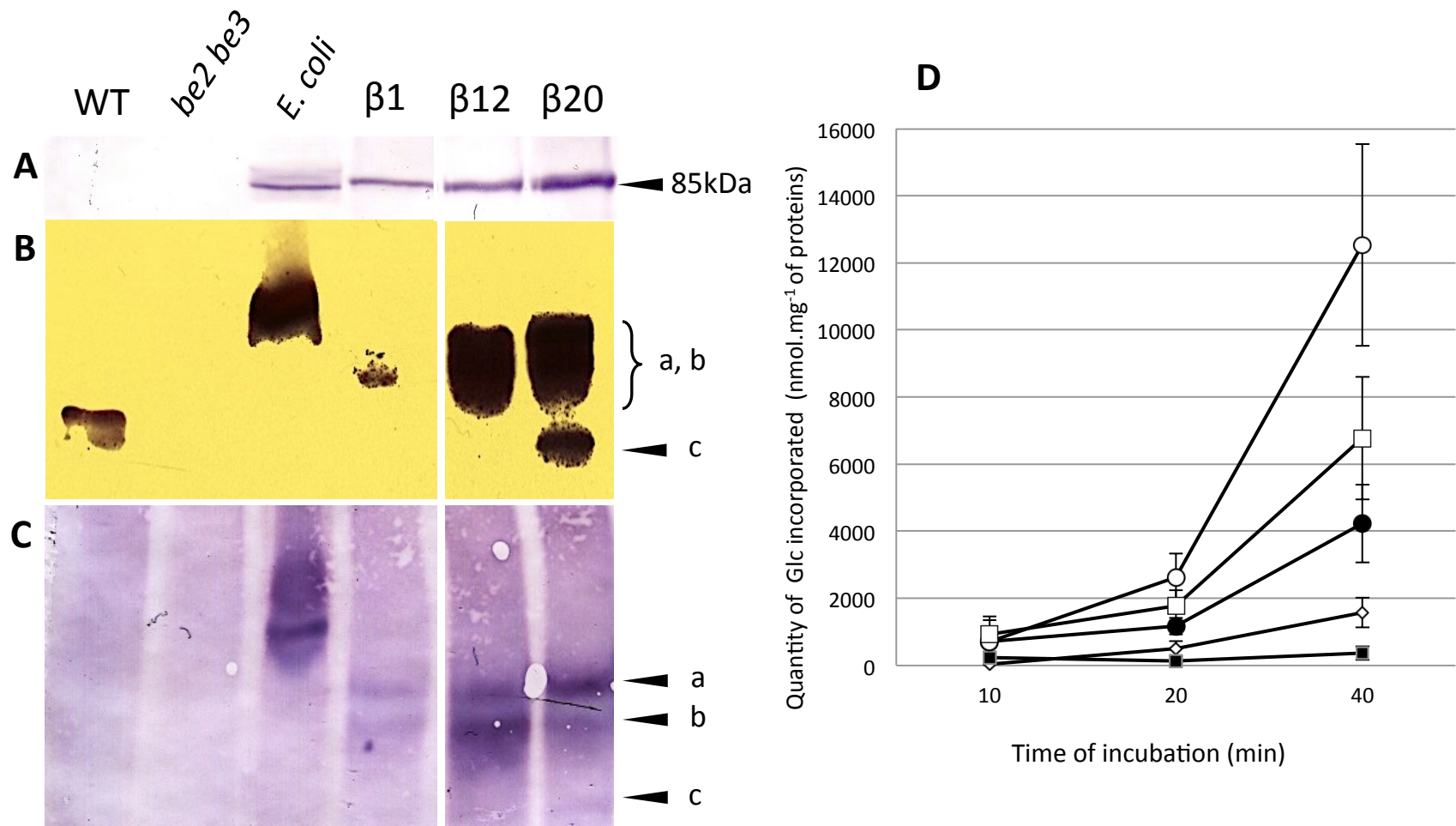


**Figure 2: Expression of *glgB* in the *be2 be3* transformed lines.** (A) Immunoblot analysis performed in denaturing conditions. Protein extracts were denatured before and during migration in the polyacrylamide gel. After migration, proteins were blotted onto a nitrocellulose membrane and hybridized with a peptide-directed antibody raised against GlgB. (B) zymogram of branching enzyme activity. The polyacrylamide gel contains DP7 maltooligosaccharides and phosphorylase “a”. Branching enzyme activity was revealed by incubating the gel for 2 hours in a phosphorylase “a” stimulating buffer. Bands of branched polyglucans were detected by soaking the gel in iodine solution. (C) Immunoblot analysis performed in non-denaturing conditions: protein extract preparation and migration in the gel was carried out as in (B). After migration, proteins were treated as in (A). WT: wild type of *A. thaliana* (*Wassilewskija* ecotype); β1, β12, β20: transgenic plants expressing GlgB; *be2 be3*: branching enzyme double mutant (Dumez et al., 2006); *E. coli*: bacterial cell extract of wild type *E. coli*. Proteins or activity bands corresponding to GlgB expressed in plants were labeled as a, b, and c. In (A), (B) and (C) all lines are from the same gel and blots. (D) *in vitro* assay of branching enzyme activity. Protein extracts were incubated for 10 to 40 min in a buffer containing DP7 maltooligosaccharides, phosphorylase “a” and [U-<sup>14</sup>C]Glc-1-P (7.4 kBq per assay) at 50 mM final concentration. The mean of incorporated Glc into branched polyglucans was calculated for 3 independent assays and plotted against the time of incubation. Vertical lines stand for standard deviation. Open diamonds: WT extract; closed squares: *be2 be3* mutant; closed circles: β1; open squares: β12; open circles: β20.

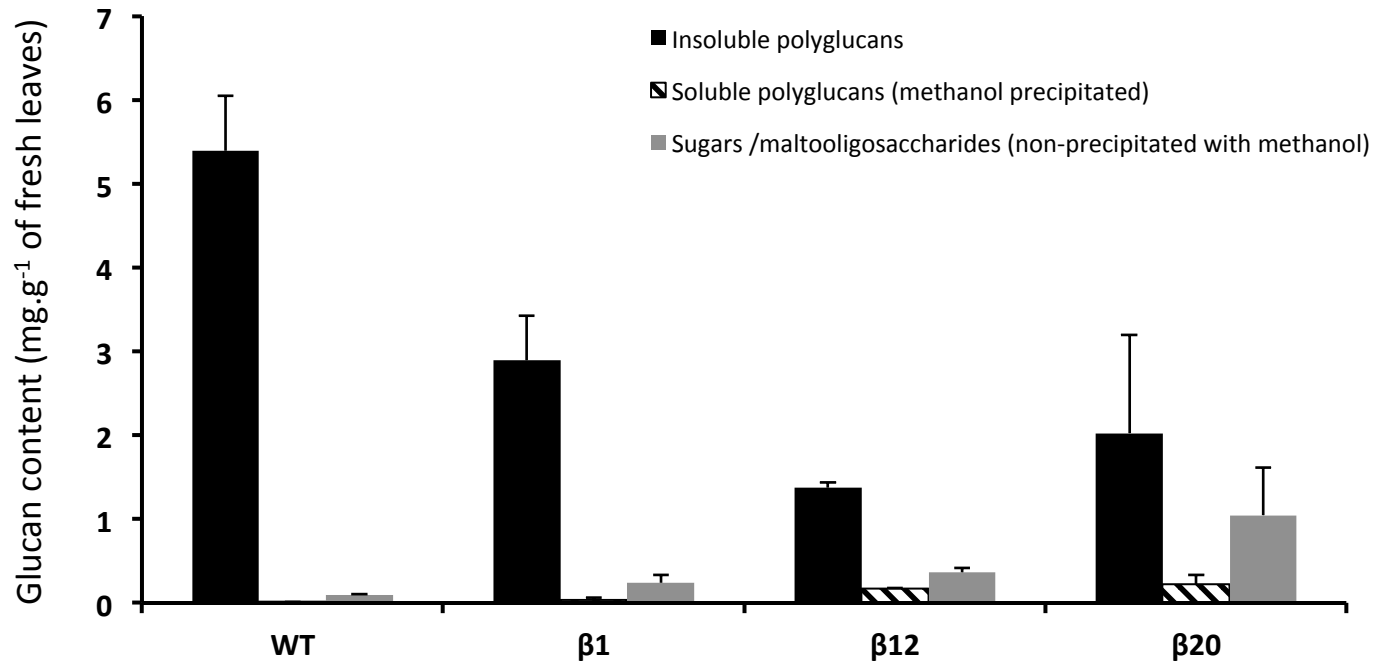


**Figure 3: Leaf glucan contents.** Glucans were extracted from leaves of 3-week old plants by the perchloric acid protocol. Leaves were harvested at the end of 16-h light period. Insoluble and soluble polyglucans and sugars/maltooligosaccharides were assayed by a spectrophotometric method. The averages of three independent cultures are presented. WT: wild type *WS* ecotype; β1, β12, β20: transgenic plants expressing the *E. coli glgB* gene. Vertical thin bars are the standard deviation of three independent biological replicates.

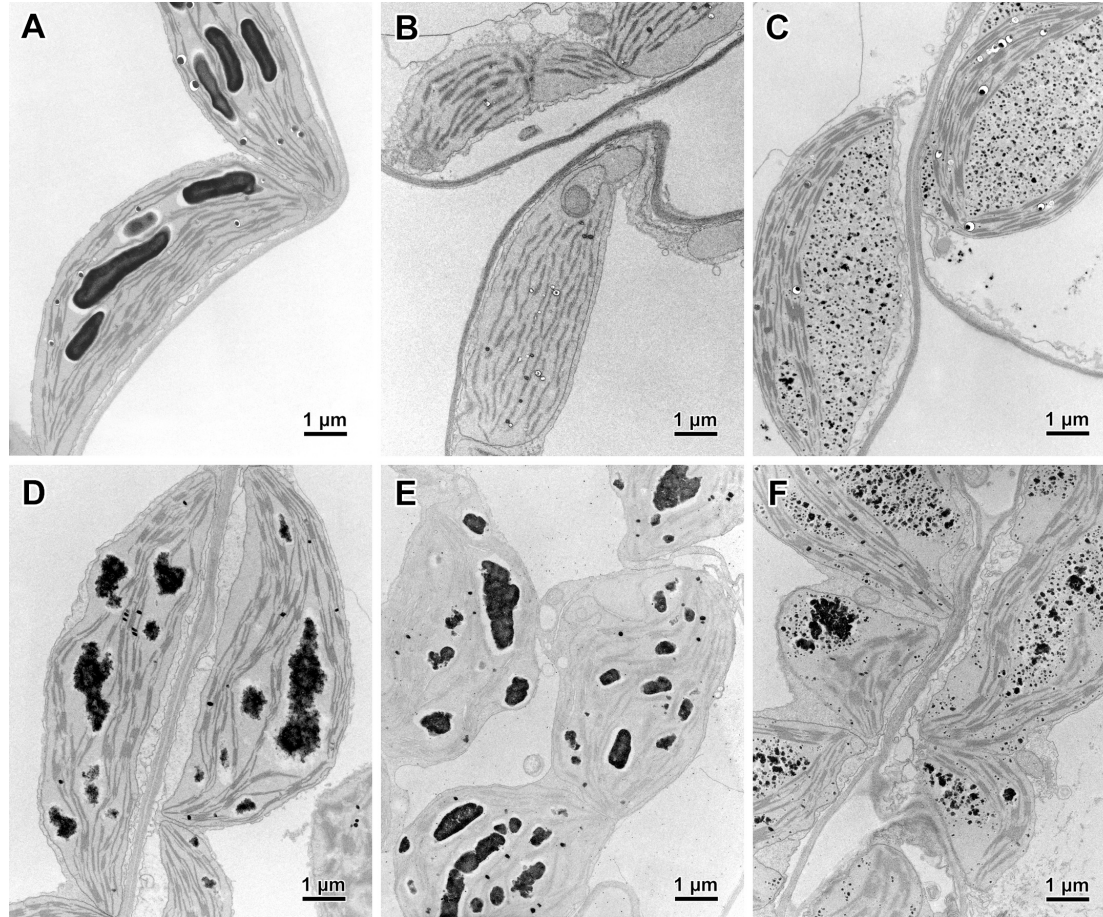


**Figure 4: Transmission electron microscopy of leaf chloroplasts.** Leaves from plants were harvested at the end of the day, cut in small strips and immediately fixed with glutaraldehyde in a cacodylate buffer and stained with PATAg to reveal glucans. A: wild type from *Wassilewskija* ecotype of *A. thaliana*; B: *be2 be3*: branching enzyme double mutant; C: *isa1 isa3 pu1*: debranching enzyme triple mutant accumulating phytoglycogen ([Wattebled et al. 2008](#)); D:  $\beta 1$ , E:  $\beta 12$ , F:  $\beta 20$ : *be2 be3* transgenic plants expressing the bacterial *glgB* gene.



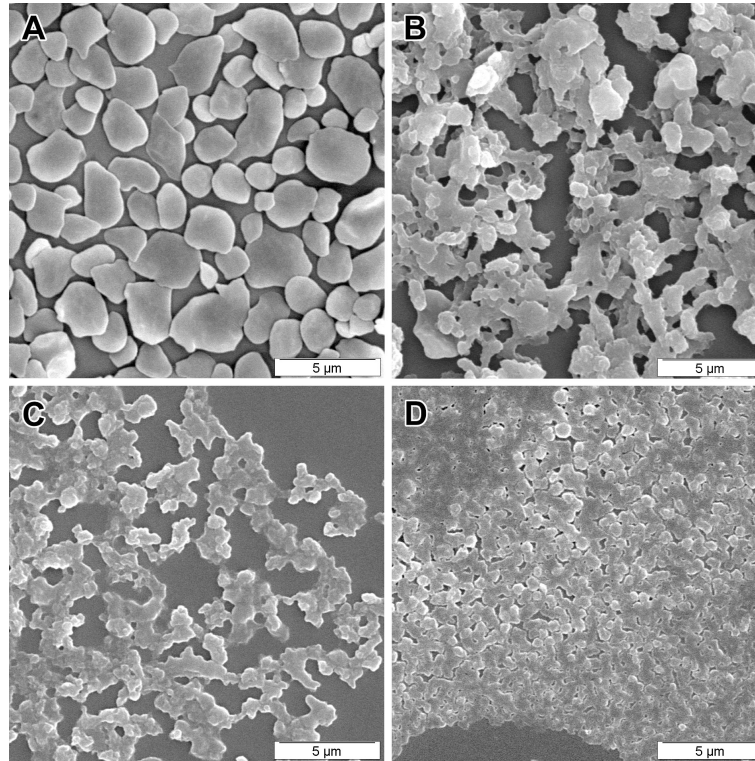


**Figure 5: Scanning electron microscopy of purified insoluble polyglucans.** Insoluble polyglucans were extracted and purified from leaves of 3-week-old plants harvested at the end of the day of 16-h light / 8-h dark cycles. A: wild type *Wassilewskija* ecotype; B:  $\beta 1$ ; C:  $\beta 12$ ; D:  $\beta 20$ .

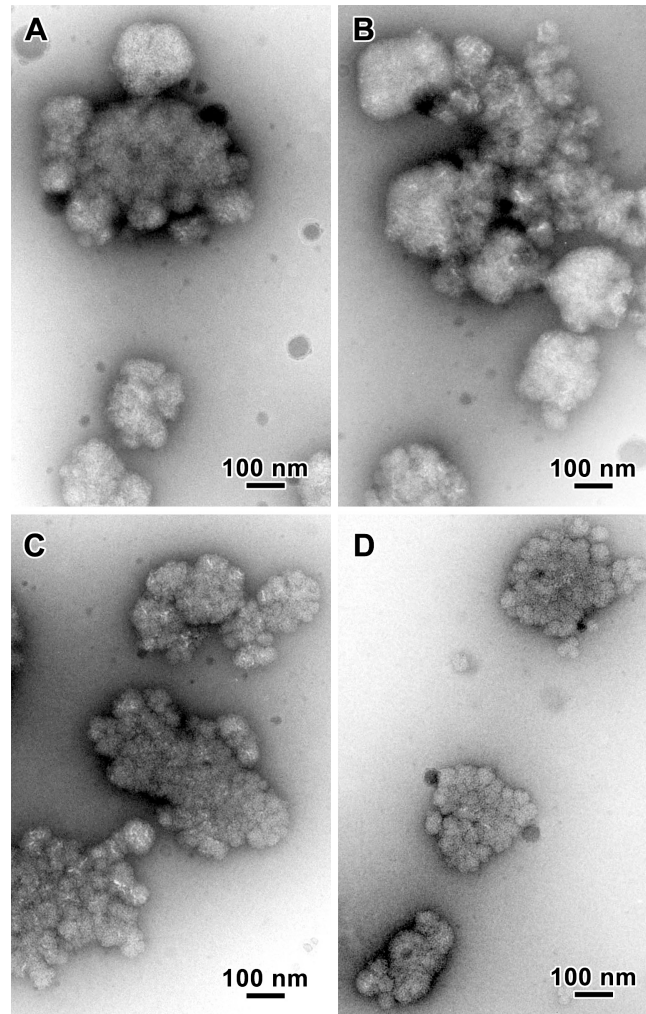


**Figure 6: Morphology of particles purified from the insoluble polyglucans of the GlgB-expressing lines.** TEM images of negatively stained particles from the insoluble fractions of  $\beta 12$  (A, B) and  $\beta 20$  (C, D).



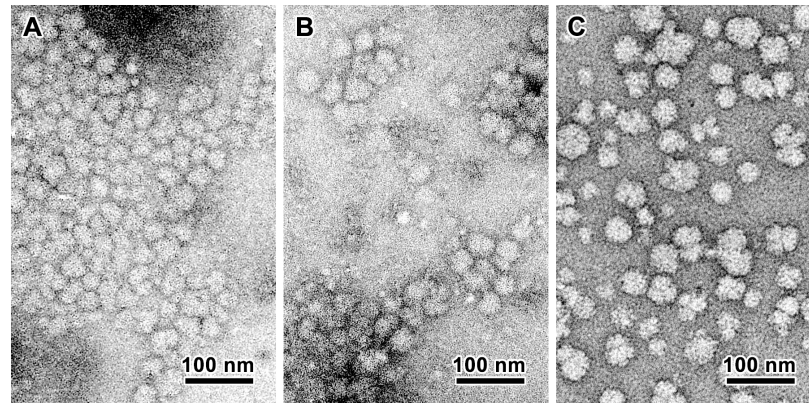


**Figure 7: Morphology of particles purified from the soluble polyglucans isolated from the GlgB-expressing lines.** TEM images of negatively stained particles from the water-soluble polyglucans isolated from  $\beta$ 12 (A) and  $\beta$ 20 (B). The image of maize phytoglycogen (C) is given for comparison.

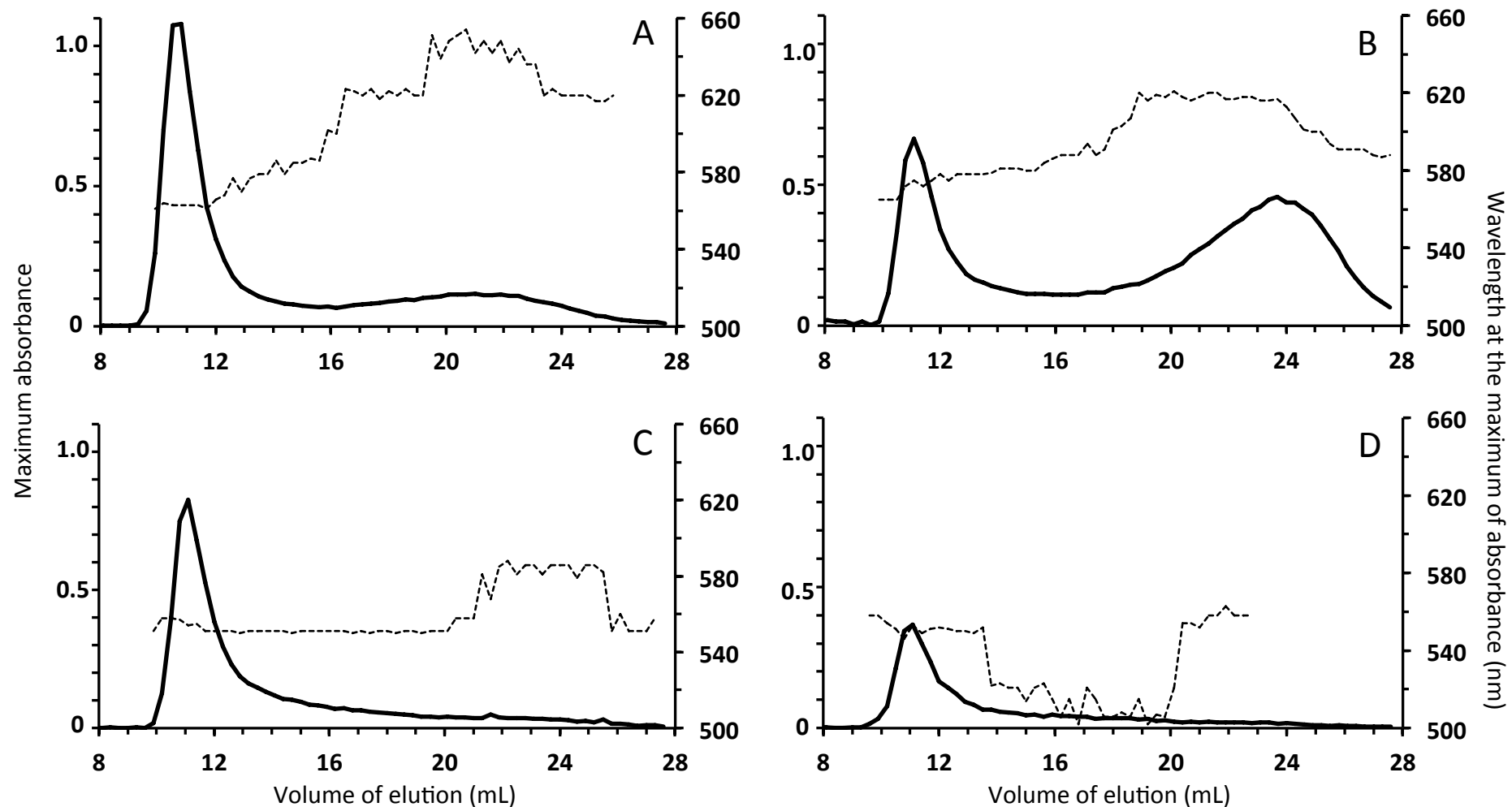


**Figure 8: Fractionation of insoluble polyglucans by size exclusion chromatography.** Purified insoluble polyglucans were dispersed in DMSO, solubilized in NaOH 10 mM and loaded onto a Sepharose® CL-2B matrix. Elution was conducted in NaOH 10 mM at a rate of 12 mL.h<sup>-1</sup>. 300  $\mu$ L fractions were collected and subsequently analyzed by iodine spectrophotometry. Thick continuous lines are the maximum absorbance of the iodine-polyglucan complexes (left Y-axis). Dashed lines indicate the wavelength (nm) of the iodine-polyglucan complex at the maximum of absorbance (right Y-axis). X-axis is the volume of elution in mL. A: WT; B:  $\beta 1$ ; C:  $\beta 12$ ; D:  $\beta 20$ .

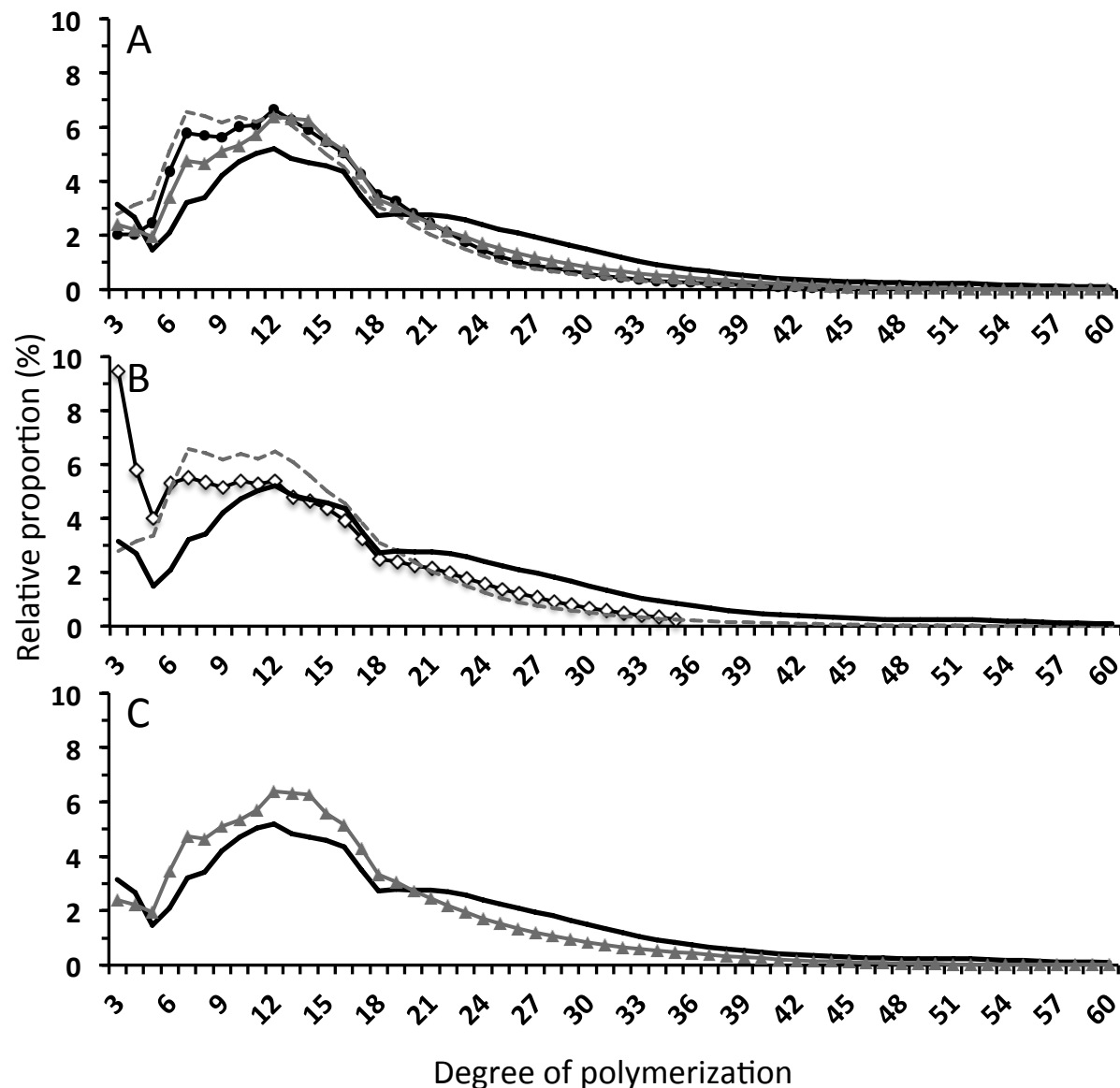
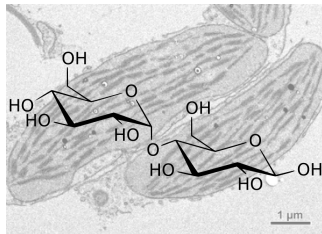


**Figure 9: Chain length distribution of insoluble polyglucans.** Purified insoluble polyglucans were digested with a mix of bacterial debranching enzymes. The corresponding linear glucans were separated by high-performance anion exchange chromatography and detected by pulsed amperometric detection (HPAEC-PAD). The fraction of each DP (from 3 to 60 glucose residues) is expressed in % of the total DP presented on the profile. (A) WT: continuous black line;  $\beta 1$ : grey triangles;  $\beta 12$ : closed circles;  $\beta 20$ : discontinuous grey line. (B) Comparison of the profiles of the WT (continuous black line) and  $\beta 20$  (discontinuous grey line). The profile of the *isa1 isa3 pu1* triple mutant already published in Wattebled et al., 2008 is given (open diamonds). (C) Comparison of the profiles of the WT (continuous black line) and  $\beta 1$  (grey triangles).

### No branching

- ⇒ no starch
- ⇒ no phytyglycogen

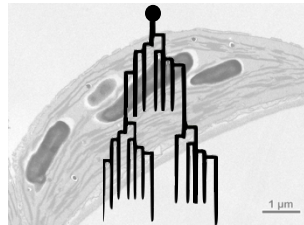


*be2 be3*

**BR/DEBR = 0**

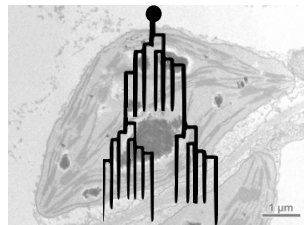
### Balanced or near-balanced branching & debranching

⇒ starch or starch-like



*WT*

**BR/DEBR = optimal**

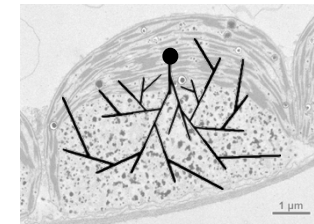


$\beta 1$

**BR/DEBR  $\approx$  optimal**

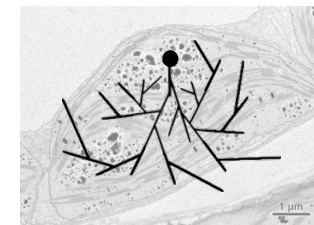
### No debranching or high branching

- ⇒ no starch
- ⇒ phytyglycogen or phytyglycogen-like insoluble polyglucan



*isa1 isa3 pu1*

**BR/DEBR =  $\infty$**



$\beta 20$

**BR/DEBR  $\gg$  optimal**

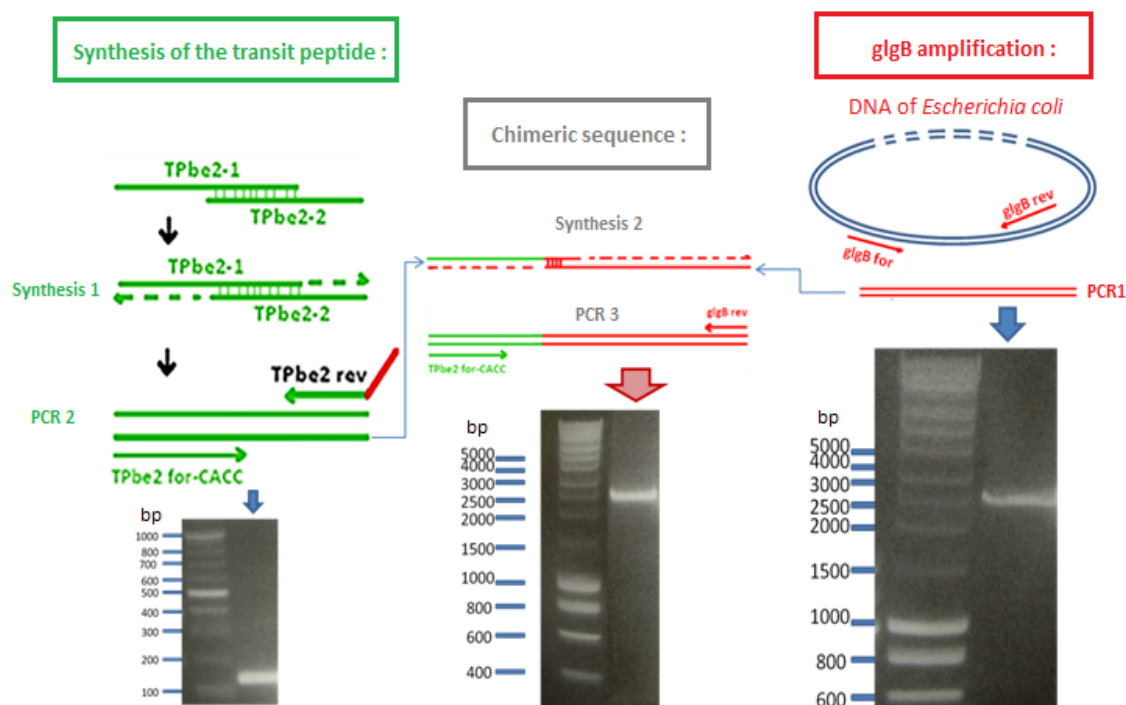
**Figure 10: Starch or starch-like polyglucan synthesis occurs thanks to a balanced branching / debranching activity ratio assuming that starch synthase activity is not limiting whatever the branching/debranching ratio.** Left panel: in the absence of branching activity (*be2 be3* double mutant), starch or phytyglycogen synthesis is impossible and is substituted by maltose accumulation; the BR/DEBR ratio is null. Middle panel: when the ratio BR/DEBR activity is balanced (WT) or near-balanced ( $\beta 1$ ), starch or starch-like polyglucan synthesis is promoted. In the case of  $\beta 1$ , the slight structural modification of starch is due to the expression of the bacterial glycogen-branching enzyme that has different catalytic and regulatory properties. Right panel: in the absence of debranching activity (such as in *isa1 isa3 pu1*; BR/DEBR is infinite) or when branching activity is extremely high (such as in  $\beta 20$ ; BR/DEBR  $\gg$  optimal) phytyglycogen or phytyglycogen-like insoluble polyglucan is synthesized respectively. Superimposed drawings correspond to (from left to right): maltose, amylopectin, phytyglycogen; black points depict the reducing end.

## Supplemental Figure S1

### Description of the approach employed for the synthesis the GlgB chimeric sequence used for expression in *A. thaliana*.

The chimeric sequence used to transform the *be2 be3* double mutant is composed of the nucleotide sequence of the transit peptide of the plant gene AtBE2 (At5g03650) and the *E. coli glgB* nucleotide sequence (M13751). a) Global scheme of the method is presented. b) Primers nucleotide sequences. Nucleotides in green correspond to the AtBE2 transit peptide sequence and nucleotides in red correspond to the coding sequence of *glgB*. Nucleotides “CACC” highlighted in blue are required for insertion of the sequence in the pENTR/D-TOPO vector. (c) Hybridization temperatures used for each couple of primers and number of cycles used during amplification. (d) Nucleotide and amino acid sequences of the chimeric gene.

#### a) Global scheme



The coding sequence of *glgB* was amplified directly with *E. coli* genomic DNA (PCR1). The transit peptide was synthesized with two long complementary primers (synthesis 1) (PCR2). PCR products 1 and 2 were hybridized to synthesize the chimeric sequence (synthesis 2) and the chimeric sequence was finally amplified (PCR 3) before its insertion in the entry vector.

## b) Primers sequences

glgB for	atgtccgatcgtatcgatagagacgtgatt
glgB rev	tcattctgctcccgaaacca
TPbe2-1	atggtggtgattcacggagtgctcttactccacgcttcactcttctctcgacctc tcaacactggctttaatgccggcaattccaccctctcttcttcttcaaaaagcacc tc
TPbe2-2	agagatagcttgtgacgaagaatcaaactccgcagattgtttccagcaaagatcttc cgagagagaggggtgctttttgaagaagaaagagaggggtgg
TPbe2 for-CACC	caccatggtggtgattcacggagt
TPbe2 rev	aatcacgtctctatcgatacgatcggacatagagatagcttgtgacgaagaatca

## c) PCR conditions

Primer couples	Hybridization temperatures	Number of cycles
PCR1: glgB for / glgB rev	61°C	34
SYNTHESIS 1: TPbe2-1 / TPbe2-2	55°C	24
PCR2: TPbe2 for-CACC / TPbe2 rev	54°C	30
SYNTHESIS 2: with amplicons from PCR1 & PCR2	54°C	20
PCR3: TPbe2 for-CACC / glgB rev	54°C	34

## d) Chimeric sequences

Nucleotide sequence of the chimeric gene

In green: nucleotides corresponding to the transit peptide of the AtBE2 gene. In red: nucleotides of the coding sequence of *E. coli glgB* gene. In blue, nucleotides required for insertion of the construction into the entry vector. Underlined nucleotides correspond to the primers used for PCR amplification (see table above)

CACCATGGTGGTGATTACGGAGTGTCTCTTACTCCACGCTTCACTCTTCCTTCTCGACCTCTCAACACTGGCTT  
TAATGCCGGCAATTCCACCCTCTCTTTCTTCTTCAAAAAGCACCTCTCTCTCGGAAGATCTTTGCTGGGAAACA  
ATCTGCGGAGTTTGATTCTTCGTACAAGCTATCTCTATGTCCGATCGTATCGATAGAGACGTGATTAACGCGCT  
AATTGCAGGCCATTTTGCGGATCCTTTTTCCGTAAGTGCATAAAACACCGCGGGACTGGAAGTCCGTGC  
CCTTTTACCGACGCTACCGATGTGTGGGTGATTGAACCGAAACCGGGCGAAACTCGAAACTGGAGTGTCT  
CGACTCACGGGATTCTTTAGCGGCGTCATTCCGCGACGTAAGAATTTTTCCGCTATCAGTTGGCTGTTGTCTG  
GCATGGTCAGCAAAACCTGATTGATGATCCTTACCGTTTTGGTCCGCTAATCCAGGAAATGGATGCCTGGCTATT  
ATCTGAAGGTACTCACCTGCGCCCGTATGAAACCTTAGGCGCGCATGCAGATACTATGGATGGCGTCACAGGTAC  
GCGTTTTCTGTCTGGGCTCAAACGCCCCGTCGGGTCTCGGTGGTTGGGCAATTCAACTACTGGGACGGTCGCCG  
TCACCCGATGCGCCTGCGTAAAGAGAGCGGCATCTGGGAAGTGTATCCCTGGGGCGCATAACGGTCAGCTCTA  
TAAATACGAGATGATTGATGCCAATGGCAACTTGGCTCTGAAGTCCGACCCTTATGCCCTTGAAGCGCAAAATGCG  
CCCGAAACCGCGTCTCTTATTTGCGGGCTGCCGAAAAGGTTGTACAGACTGAAGAGCGCAAAAAAGCGAATCA  
GTTTGTATGCGCAATCTCTATTTATGAAGTTACCTGGGTTCTGGCGTCGCCACACCGACAACAATTTCTGGTT  
GAGTACCGCGAGCTGGCCGATCAACTGGTGCCTTATGCTAAATGGATGGGCTTTACCCACCTCGAACTACTGCC  
CATTAAAGAGCATCCCTTCGATGGCAGTTGGGGTTATCAGCCAACCGGCCCTGTATGCGCCAACCGCCGTTTTGG  
TACTCGCGACGACTTCCGTTATTTATTGATGCCGACACGCAGCTGGTCTGAACGTGATTCTCGACTGGGTGCC  
AGGCCACTTCCGACTGATGACTTTGCGCTTGCCGAATTTGATGGCACGAACTTGTATGAACACAGCGATCCGCG

TGAAGGCTATCATCAGGACTGGAACACGCTGATCTACAACCTATGGTCGCCGTGAAGTCAGTAACTTCCTCGTCGG  
TAACGCGCTTTACTGGATTGAACGTTTTGGTATTGATGCGCTGCGCGTCGATGCGGTGGCGTCAATGATTTATCG  
CGACTACAGCCGTAAAGAGGGGGAGTGGATCCCGAACGAATTTGGCGGGCGCGAGAATCTTGAAGCGATTGAATT  
CTTGCGTAATACCAACCGTATTCTTGGTGAGCAGGTTTTCCGGTGCGGTGACAATGGCTGAGGAGTCTACCGATTT  
CCCTGGCGTTTCTCGTCCGAGGATATGGGCGGTCTGGGCTTCTGGTACAAGTGGAACCTCGGCTGGATGCATGA  
CACCTGGACTACATGAAGCTCGACCCGGTTTATCGTCAGTATCATCACGATAAACTGACCTTCGGGATTCTCTA  
CAACTACACTGAAAACCTTCGTCTGCCGTTGTGCGATGATGAAGTGGTCCACGGTAAAAAATCGATTCTCGACCG  
CATGCCGGGCGACGCATGGCAGAAATTCGCGAACCTGCGCGCCTACTATGGCTGGATGTGGGCATTCCCGGGCAA  
GAACTACTGTTTCATGGGTAAACGAATTTGCCAGGGCCGCGAGTGGAACCATGACGCCAGCCTCGACTGGCATCT  
GTTGGAAGGCGGCGATAACTGGCACCACGGTGTCCAGCGTCTGGTGCGCGATCTGAACCTCACCTACCGCCACCA  
TAAAGCAATGCATGAAGTGGATTTTGACCCGTACGGCTTTGAATGGCTGGTGGTGGATGACAAAGAACGCTCGGT  
GCTGATCTTTGTGCGTCGCGATAAAGAGGGTAACGAAATCATCGTTGCCAGTAACTTTACGCCGGTACCGCGTCA  
TGATTATCGCTTCGGCATAAACCAGCCGGGCAAATGGCGTGAAATCCTCAATACCGATTCCATGCACTATCACGG  
CAGTAATGCAGGCAATGGCGGCACGGTACACAGCGATGAGATTGCCAGCCACGGTCGTGAGCATTCACTAAGCCT  
GACGCTACCACCGCTGGCCACTATCTGGCTGGTTCCGGAGGCAGAATGA

Aminoacid sequence of the chimeric GlgB protein (transit peptide in green)

MVVIHGVSLTPRFTLPSRPLNTGFNAGNSTLSFFFKKHPLSRKIFAGKQSAEFDS  
SSQAIMSDRIDRDVINALIAGHFADPFVSLGMHKTTAGLEVRALLPDATDVWVI  
EPKTGRKLAKLECLDSRGFFSGVIPRRKNFFRYQLAVVWHGQONLIDDPYRFGPL  
IQEMDAWLLSEGTHLRPYETLGAHADTMDGVTGTRFSVWAPNARRVSVVGQFNYW  
DGRRHMPMLRKESGIWELFIPGAHNGQLYKYEMIDANGNLRLKSDPYAFEAQMRP  
ETASLICGLPEKVVQTEERKKANQFDAPISIEVHLGSWRRHTDNNFWLSYRELA  
DQLVPYAKWMGFTHLELLPINEHPFDGSWGYQPTGLYAPTRRFGTRDDFRYFIDA  
AHAAGLNVILDWVPGHFPTDDFALAEFDGTNLYEHSDPREGYHQDWNTLIYNYGR  
REVSNFLVGNALYWIERFGIDALRVDAVASMIYRDYSRKEGEWIPNEFGGRENLE  
AIEFLRNTNRILGEQVSGAVTMAEESTDFPGVSRPQDMGGLGFWYKWNLGWMHDT  
LDYMKLDPVYRQYHHDKLTFGILYNYTENFVLPLSHDEVVHGKKSILDRMPGDAW  
QKFANLRAYYGWMWAFPGKKLLFMGNEFAQGREWNHDASLDWHLLEGGDNWHHGV  
QRLVRDLNLTyrHHKAMHELDfDPYGFewLVDDKERSVLIFVRRDKEGNEIIVA  
SNFTPVPRHDYRFGINQPGKWREILNTDSMHYHGsnAGNGGTVHSDEIASHGRQH  
SLSLTLPLPLATIWLvREAE

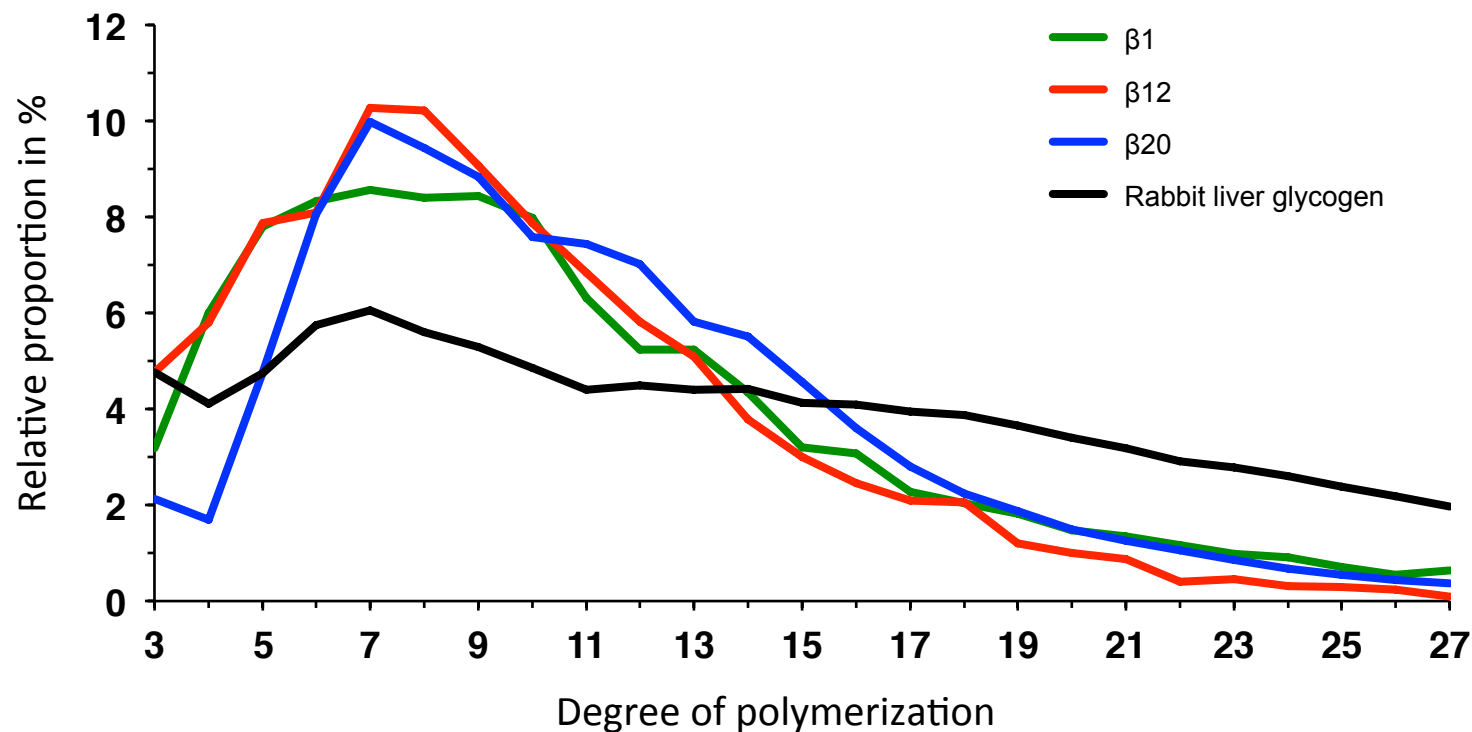


WS

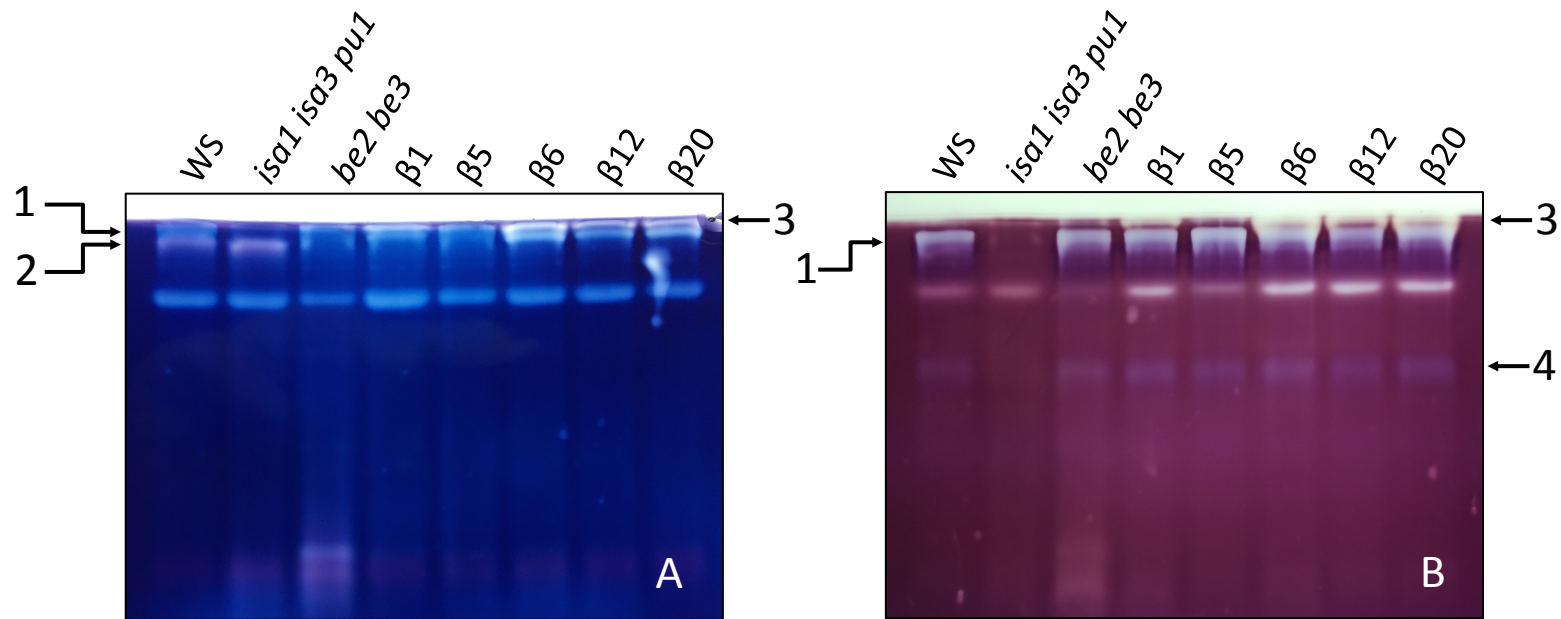
*be2 be3* $\beta 1$  $\beta 5$  $\beta 6$  $\beta 12$  $\beta 20$ 

**Supplemental Figure S2: comparison of mature plant size.** Seeds were sown on peat-based compost and plants were grown in greenhouse for 16h in the light at 21°C and 8h in the dark and 16°C. Pictures were taken 3 weeks after germination. The *be2 be3* double mutant has a strong growth retardation phenotype and plants are much smaller than wild type (Dumez et al., 2006) whereas all transformed plants expressing *E. coli* GlgB branching enzyme have a phenotype close to that of the wild type reference.

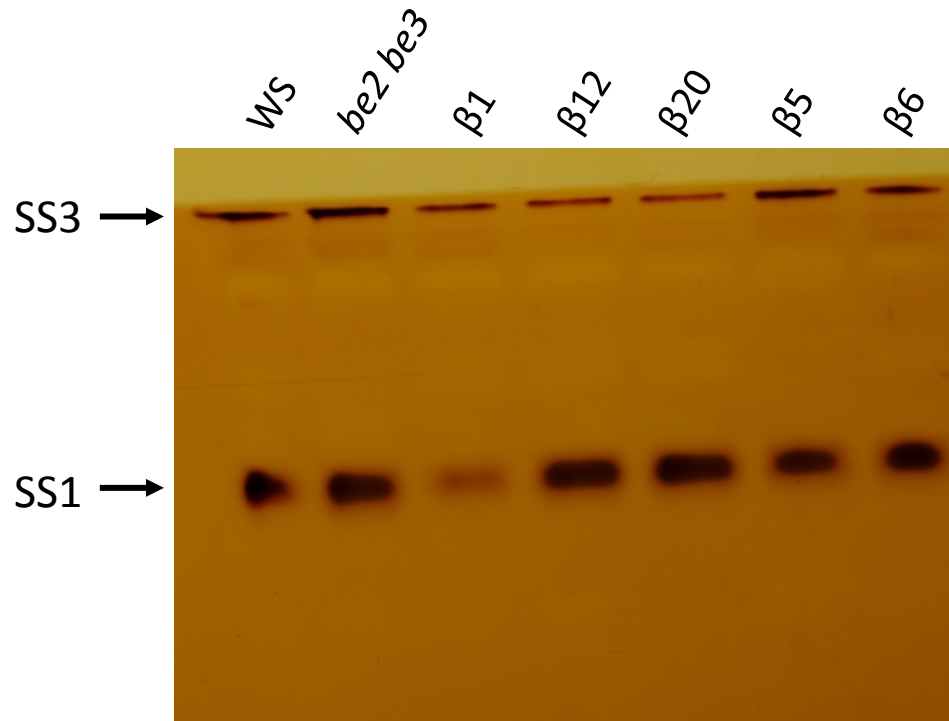




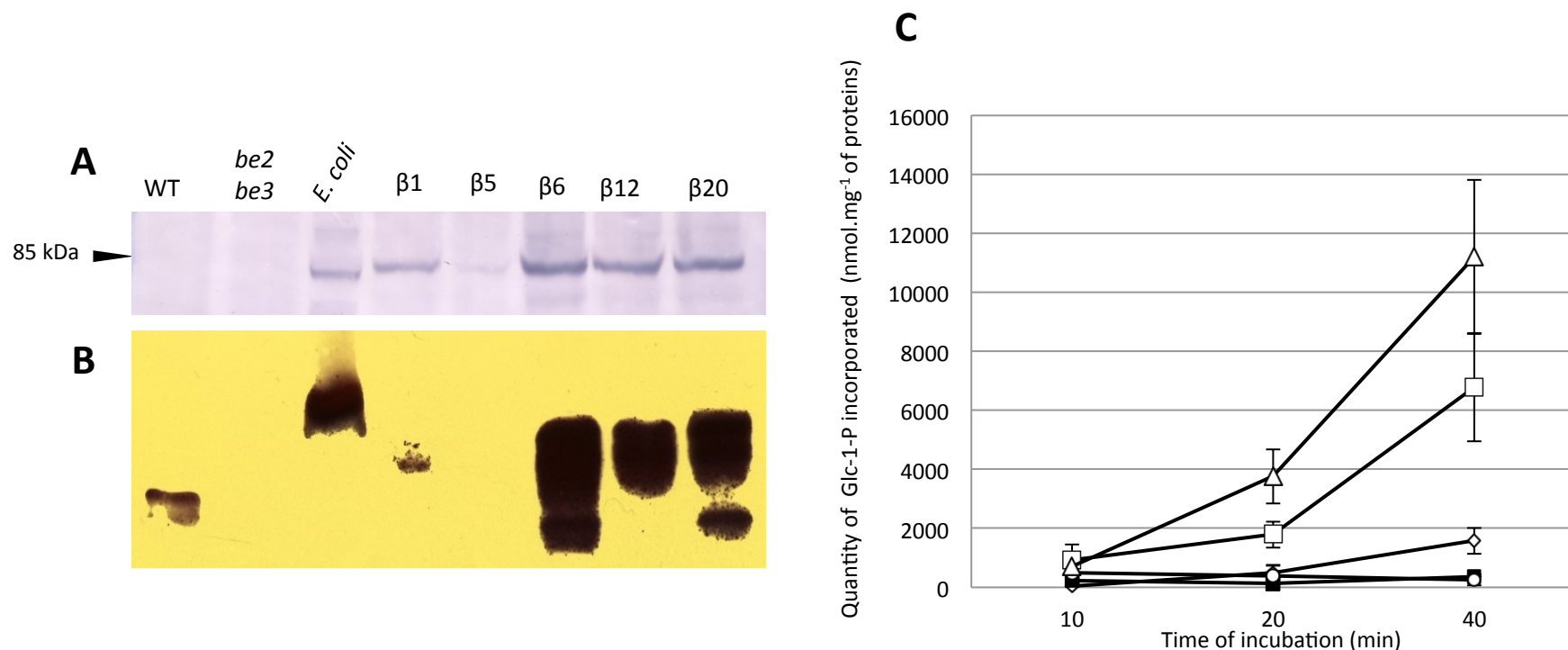
**Supplemental Figure S3: Chain length distribution profiles of water soluble polyglucans** purified from GlgB-expressing lines  $\beta 1$  (green),  $\beta 12$  (red) and  $\beta 20$  (blue) compared to that of the rabbit liver glycogen (black). After purification, water soluble polyglucans were debranched by a mix of bacterial isoamylase and pullulanase. The branched products were analyzed by HPAEC-PAD. The relative proportion of each glucan is plotted versus their degree of polymerization. Values are the mean of two analysis carried out with soluble polyglucans extracted of plants cultivated independently.



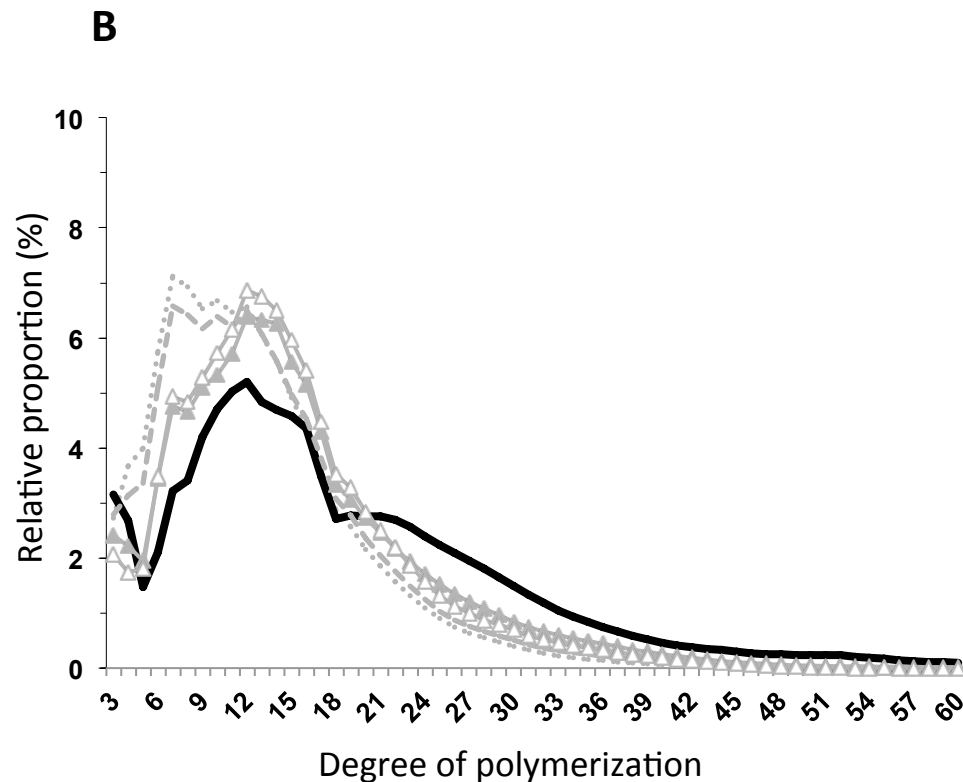
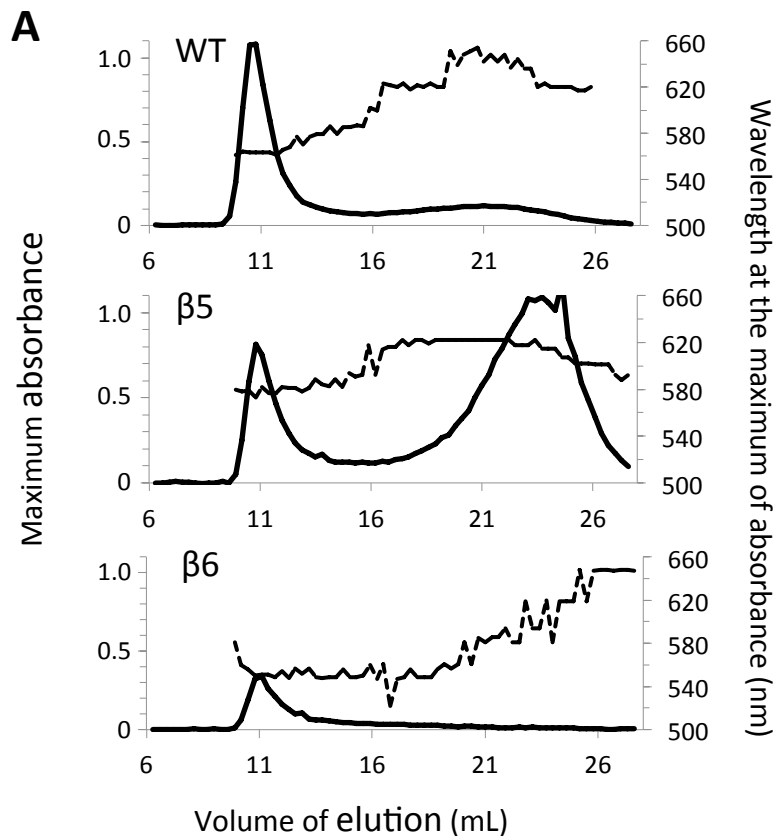
**Supplemental Figure S4: Zymogram analysis of transformed plant expressing GlgB.** Three to four leaves of 3 week-old plants were harvested at mid-day for soluble extract preparation. The equivalent of 50  $\mu$ g of proteins were loaded on polyacrylamide gel impregnated with either 0.3% of potato soluble starch (A) or 0.3% of maize  $\beta$ -limit dextrins (B). After migration (2 h at 4°C, 15 mA / gel), the gels were incubated overnight at room temperature in a buffer composed of : Tris 25 mM; Glycine 192 mM;  $MgCl_2$  1 mM;  $CaCl_2$  1 mM; DTT 10 mM. After incubation, enzymes that modified the substrate were revealed by soaking the gels in iodine solution (1% KI [w/v]; 0.1%  $I_2$  [w/v]). The gels were rinsed in water before taking pictures. WS is the wild type reference (*Wassilewskija*) and all other plants are in the same genetic background. *be2 be3* corresponds to a double mutant lacking endogenous branching enzymes.  $\beta_1$ ,  $\beta_5$ ,  $\beta_6$ ,  $\beta_{12}$ , and  $\beta_{20}$  are *be2 be3* mutants expressing different levels of *E. coli* GlgB. Blue Band labeled 1 and red band labeled 2 were previously determined as Iso1 and BE2 respectively (Dumez et al., 2006; Wattebled et al., 2008). The pale pink band labeled 3 with an extremely low mobility, present only in transformed plants, corresponds to GlgB. Band 4 is the pullulanase (Wattebled et al., 2008).



**Supplemental Figure S5: Zymogram analysis of soluble starch synthases activities.** An equal amount of proteins from leaf crude extracts was loaded on native PAGE containing 0.3% (w/v) of rabbit liver glycogen. Approximately 2h30 of migration in native conditions (Tris-glycine buffer 1X, 4°C) was applied. After incubation in an appropriate buffer for starch synthase activity (Glycyl-glycine 66 mM (pH 7.5);  $(\text{NH}_4)_2\text{SO}_4$  66 mM;  $\text{MgCl}_2$  1 mM;  $\beta$ -mercaptoethanol 3.3 mM; ADP-glucose 1.2 mM), the gel was washed 6 times into water to remove  $\beta$ -mercaptoethanol and further incubated in iodine solution until revelation of bands of activity. This zymogram is representative of three biological independent experiments.



**Supplemental Figure S6 : Expression of *glgB* in the *be2 be3* transformed lines.** (A) Immunoblot analysis performed in denaturing conditions. Protein extracts were denatured before and during migration in the polyacrylamide gel. After migration, proteins were blotted onto a nitrocellulose membrane and hybridized with a peptide-directed antibody raised against GlgB. (B) zymogram of branching enzyme activity. The polyacrylamide gel contains DP7 maltooligosaccharides and phosphorylase “a”. Branching enzyme activity was revealed by incubating the gel for 2 hours in a phosphorylase “a” stimulating buffer. Bands of branched polyglucans were detected by soaking the gel in iodine solution. (C) *in vitro* assay of branching enzyme activity. Protein extracts were incubated for 10 to 40 min in a buffer containing DP7 maltooligosaccharides, phosphorylase “a” and [U-<sup>14</sup>C]Glc-1-P (7.4 kBq per assay) at 50 mM final concentration. The mean of incorporated Glc into branched polyglucans was calculated for 3 independent assays and plotted against the time of incubation. Vertical lines stand for standard deviation. Open diamonds: WT extract; closed squares: *be2 be3* mutant; open squares:  $\beta 12$ ; open circles:  $\beta 5$ ; open triangles:  $\beta 6$ .



**Supplemental Figure S7 : Structure of polysaccharides produced in  $\beta 5$  and  $\beta 6$  transformant lines.**

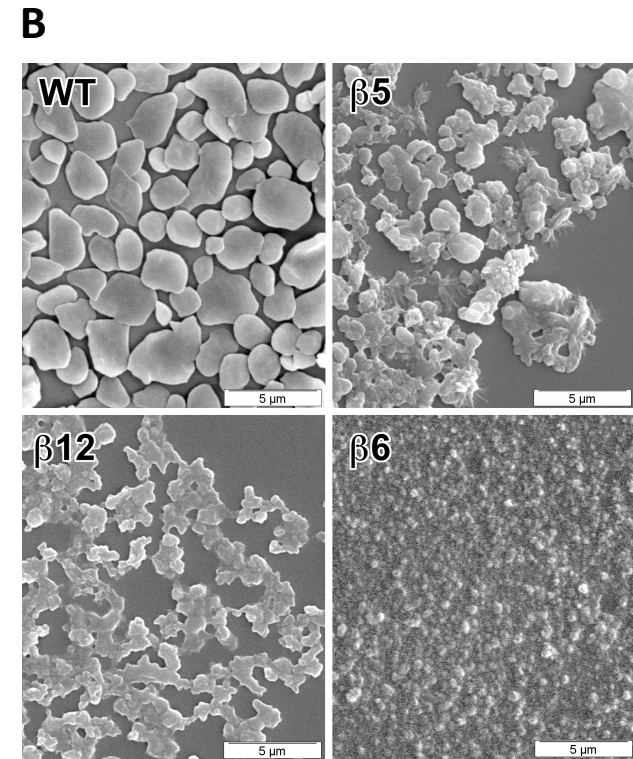
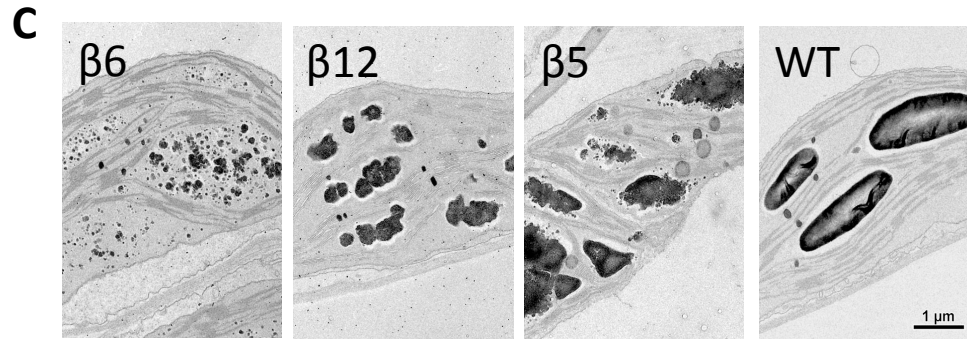
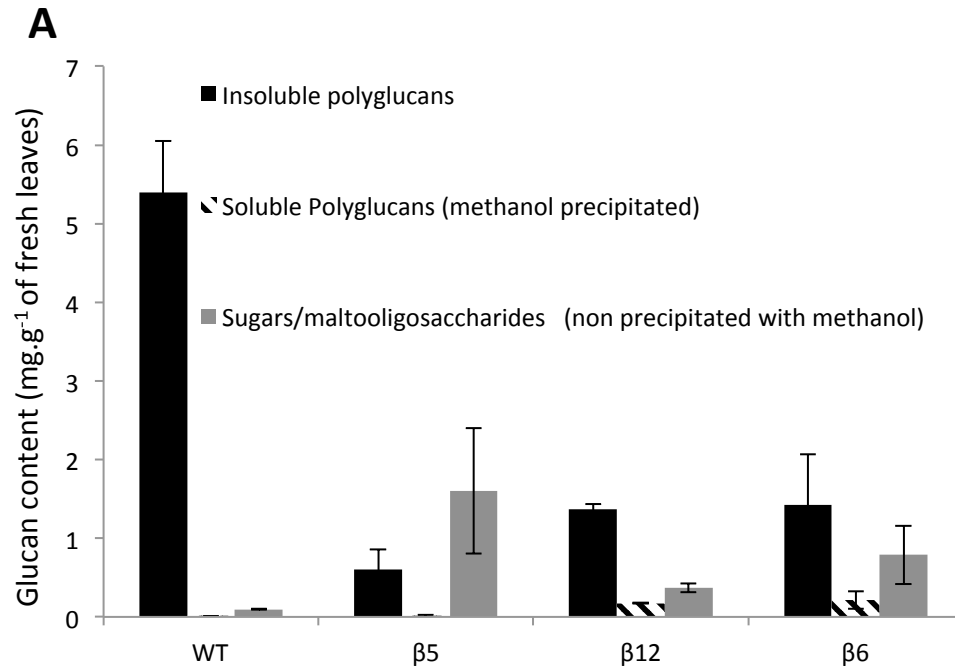
**(A) Fractionation of insoluble polyglucans by size exclusion chromatography.** Dashed lines indicate the wavelength (nm) of the iodine-polyglucan complex at the maximum of absorbance (right Y-axis).

**(B) Chain length distribution of insoluble polyglucans.** WT: continuous black line;  $\beta 1$ : closed grey triangles;  $\beta 5$ : open grey triangles ;  $\beta 6$ : dotted grey line;  $\beta 20$ : discontinuous grey line.

**(C) Structural parameters of polysaccharides produced in  $\beta 5$  and  $\beta 6$  tranformant lines.** The branching degree was calculated according to Szydlowski et al. (2011).

**C**

Sample	WT	$\beta 5$	$\beta 12$	$\beta 6$
Branching degree (%)	5.1	6.2	6.8	7.8
$\lambda_{\max}$ of amylopectin (nm)	563	571	553	545
Crystallinity index (%)	33	23	20	15



**Supplemental Figure S8 : Leaf glucan contents and granules morphology.**

A: For glucan content the average of three independent cultures are presented. Vertical thin bars are the standard deviation of three independent biological replicates. B: Scanning electron microscopy images of purified insoluble polyglucans. C: Transmission electron microscopy images of leaf chloroplasts positively stained with PATAg.